FRACTALKINE SIGNALING IN PSYCHIATRIC DISORDER: OBSERVATIONS IN THE POSTMORTEM BRAIN

by

Sarah Louise Hill

B.Sc., The University of California, Santa Cruz, 2015

A THESIS SUBMITTED IN PARTIAL FULFILLMENT OF

THE REQUIREMENTS FOR THE DEGREE OF

MASTER OF SCIENCE

in

THE FACULTY OF GRADUATE AND POSTDOCTORAL STUDIES

(Neuroscience)

THE UNIVERSITY OF BRITISH COLUMBIA

(Vancouver)

October 2019

The following individuals certify that they have read, and recommend to the Faculty of Graduate and Postdoctoral Studies for acceptance, a thesis/dissertation entitled:

Fractalkine Signaling in Psychiatric Disorder: Observations in the Postmortem Brain

submitted by Sarah L. Hill in partial fulfillment of the requirements for

the degree of Master of Science

in Neuroscience

Examining Committee:

Clare Beasley, Psychiatry
Supervisor

William Honer, Psychiatry
Supervisory Committee Member

Supervisory Committee Member

Annie Ciernia, Biochemistry
Additional Examiner

Additional Supervisory Committee Members:

Alasdair Barr, Pharmacology
Supervisory Committee Member

Supervisory Committee Member

Abstract

Schizophrenia (SCZ), bipolar disorder (BD), and major depressive disorder (MDD) are debilitating psychiatric illnesses. Though the pathophysiology underlying each disorder is not yet understood, previous studies have suggested that altered immune function may play a role, with microglia, the brain's resident immune cells, implicated in this process. A recent genetic association study and meta-analysis of microarray data indicated that dysregulation of CX3CR1, a microglial G-protein coupled receptor, may be associated with SCZ. Signaling between CX3CR1 and its neuronal ligand, fractalkine (CX3CL1), is proposed to mediate neuron-microglia interactions, recruiting microglia to synaptic sites and modulating changes in microglial activation status. However, it remains to be determined whether fractalkine is dysregulated in SCZ, BD, or MDD, or if fractalkine signaling is associated with microglial morphology and activation status, or synaptic density in these disorders. To this end, we quantified mRNA and protein expression of fractalkine, CX3CR1, and the disintegrin-like metalloproteinase 10 (ADAM10), involved in ectodomain shedding of fractalkine, in postmortem brain tissue from individuals with SCZ, BD, MDD and matched controls. We detected a significant decrease in fractalkine protein levels in SCZ relative to controls, suggesting fractalkine-CX3CR1 signaling may be disrupted in this disorder. Correlations were observed between fractalkine, CX3CR1, microglial measures and pre-synaptic protein levels.

Lay Summary

Schizophrenia (SCZ), bipolar disorder (BD), and major depressive disorder (MDD) are severe mental illnesses. While the origins of each disorder are unknown, accumulating evidence suggests altered immune function may play a role. In the brain, the immune response is carried out by specialized cells called microglia. Though the various functions of these cells are not fully understood, previous research has indicated abnormal microglial activity may be a feature of SCZ, BD, and MDD. In the present study, we measured levels fractalkine, CX3CR1, and ADAM10, three immune-related molecules known to mediate microglial function, in the postmortem brain of SCZ, BD, MDD, and control individuals. Levels of fractalkine were significantly diminished in SCZ, providing further evidence of altered microglial activity and abnormal immune function in this disorder.

Preface

S. Hill, L. Shao, and C. Beasley each contributed to the present study. S. Hill quantified levels of fractalkine, CX3CR1, and ADAM10 in experimental subjects through ddPCR and immunoblotting and carried out statistical analyses. L. Shao carried out immunoblotting tests in white and grey matter homogenates and assisted with troubleshooting of experiments. C. Beasley designed the study.

Chapters 3.1.5, 3.1.7, 3.2.5, and 3.3.5 are based on a previous study carried out in our lab by C. Hercher, A. Ypsilanti, L. Toker, and C. Beasley. C. Hercher carried out immunostaining of the Array Collection tissue samples and quantified corresponding microglial measures. A. Ypsilanti measured protein levels of SNAP-25 and MBP in the Array Collection subjects. L. Toker carried out statistical analyses. C. Beasley designed the study. Using protein and microglial measures from this previous study, S. Hill carried out further statistical analyses to examine correlations with data from the present study.

Chapters 3.1.6, 3.1.7, 3.2.6, and 3.3.5 are based on prior work carried out under W. Honer. Using measures of pre-synaptic protein levels quantified in his lab, S. Hill carried out further statistical analyses to examine correlations with data from the present study.

The present study was approved by UBC C&W Research Ethics Board (#H10-00775).

Table of Contents

List of Tables

List of Figures

List of Abbreviations

1X: one time

4X: four times

5X: five times

αFKN: anti-fractalkine antibody

μg: micrograms

μL: microliters

AA: amino acid

ACC: anterior cingulate cortex

AMPA: α-amino-3-hydroxy-5-methyl-4-isoxazolepropionic acid

AD: Alzheimer's disease

ADAM10: A Disintegrin and Metalloproteinase 10

ADAM17: A Disintegrin and Metalloproteinase 17

ALS: amyotrophic lateral sclerosis

ANCOVA: Analysis of covariance

ANOVA: Analysis of variance

Arg: Arginine

ATP: Adenosine triphosphate

BBB: blood-brain barrier

BD: bipolar disorder

BMI: body mass index

cDNA: complementary deoxyribonucleic acid

CNS: central nervous system

CON: control

Cp: crossing point

CPLX1: complexin-I

CPLX2: complexin-2

ddPCR: Droplet digital polymerase chain reaction

DSM: Diagnostic and Statistical Manual of Mental Disorders

CRP: C-reactive protein

CX3CL1: CX_3C ligand 1

CX3CR1: CX_3C receptor 1

DLPFC: dorsolateral prefrontal cortex

ELISA: enzyme-linked immunosorbent assay

FKN: fractalkine

GABA: γ-aminobutyric acid

$GABA_A$: γ-aminobutyric acid type A receptor

Gln: Glutamine

Gt: goat

HLA-DR: human leukocyte antigen DR

HRP: horseradish peroxidase

IBA-1: ionized calcium-binding adaptor molecule 1

IL-1β: interleukin-1β

IL-6: interleukin-6

IL-10: interleukin-10

kDa: kilodaltons

KO: knock-out

LPS: lipopolysaccharide

MBP: myelin basic protein

MCP-1: Monocyte chemoattractant protein-1

MDD: major depressive disorder

MDD+Psychosis: depression with psychosis

MDD-Psychosis: depression without psychosis

mg: milligrams

mL: milliliters

mm: millimeters

MMP-3: matrix metalloproteinase-3

mRNA: Messenger RNA

Ms: mouse

ng: nanograms

nM: nanomolar

NMDA: N-methyl-D-aspartic acid

NMDAR: N-methyl-D-aspartic acid receptor

No.: number

PANSS: Positive and Negative Syndrome Scale

PD: Parkinson's disease

PET: positron emission tomography

PMI: postmortem interval

PVDF: polyvinylidene fluoride

qPCR: quantitative polymerase chain reaction

Rb: rabbit

rcf: relative centrifugal force

RNA: Ribonucleic acid

RIN: RNA integrity number

RT-PCR: reverse transcription polymerase chain reaction

SCZ: schizophrenia

SD: standard deviation

SEPT: Septin-5

siRNA: small interfering RNA

SMRI: Stanley Medical Research Institute

SNAP-25: Synaptosomal nerve-associated protein 25

STX: syntaxin

SYPH: synaptophysin

SYT: synaptotagmin

TACE: tumor necrosis factor alpha converting enzyme

TBP: TATA-binding protein

TBS: tris-buffered saline

TBST: tris-buffered saline with Tween-20

Thr: Threonine

TNFα: tumor necrosis factor-α

TREM2: Triggering receptor expressed on myeloid cells 2

TSPO: translocator protein

UTP: Uridine-5'-triphosphate

UTR: untranslated region

V: volts

VAMP: Vesicle-associated membrane protein

ZO-1: Zonula occludens-1

Acknowledgements

First, I thank Dr. C. Beasley for her mentorship and support. Dr. Beasley, I am tremendously grateful for your vision, your careful evaluation of data, and your kindheartedness. You are a pioneer in our field and a remarkable role model. I thank The Brain and Behavior Research Foundation for supporting this project and recognizing the importance of postmortem work. I wish to acknowledge members of my supervisory committee, Dr. W. Honer and Dr. A. Barr, for their time, their guidance, and their encouragement. To my friends and colleagues at BCMHSUS, please accept my deepest thanks for the joy you have brought me each day in lab. Li, there is nothing I can say that will convey the extent of my gratitude to you. I could not have completed this degree without you and you are an inspiration to me, both personally and professionally. Christa, I have never befriended anyone so quickly or easily before and I cherish our time together. Thank you for the laughs over tea and for liking me despite my being awful at yoga. Jehan, I know few people who work as hard as you and your strength will take you far in life. Our friendship, founded initially out of a shared appreciation of desserts, has meant the world to me these past two years. Finally, I will forever be indebted to my parents for their love and support throughout my continued education. Their examples have encouraged me to live life by my own values and have instilled in me a love of learning.

Dedication

For Zak, who has been my rock through all of this.

Chapter 1: Introduction

1.1 Major Mental Illness

1.1.1 Schizophrenia

Schizophrenia (SCZ) is a devastating psychiatric illness with typical onset during the late teens to mid-twenties[1]. Despite a prevalence of just less than 1% of the global population, the disorder is one of the top fifteen leading causes of disability worldwide[2,3]. According to the DSM-5[4], two or more of the following symptoms must be present for a diagnosis of SCZ, including either delusions, hallucinations or disorganized speech:

1) delusions;
2) hallucinations;
3) disorganized speech;
4) grossly disorganized or catatonic behavior;
5) negative symptoms.

Additional diagnostic criteria of SCZ include a marked decline in level of functioning for a significant portion of time since onset, and continuous signs of the disturbance that persist for at least 6 months[4].

1.1.2 Bipolar Disorder

Bipolar disorder (BD) is a severe mood disorder with an estimated lifetime prevalence rate of 2.2% in Canada[5]. Also a highly complex, heterogeneous mental illness, BD comprises bipolar I disorder, bipolar II disorder, and other specified and unspecified forms of the

disorder broadly characterized by periods of mania or hypomania and depression[6]. Similar to SCZ, onset of BD occurs generally in young adulthood, though an average 5.8 year delay between initial disease onset and diagnosis has been reported[7]. According to the DSM-5[4], diagnostic criteria for bipolar I disorder include presence of at least one manic episode. While periods of hypomania or depression are not required for a bipolar I diagnosis, either or both are often present in the disorder. In contrast, a bipolar II diagnosis is made when criteria have been met for at least one hypomanic episode and at least one major depressive episode, but there has never been a manic episode[4].

1.1.3 Major Depressive Disorder

Major Depressive Disorder (MDD) affects approximately 6% of the adult population worldwide, being diagnosed twice as often in women than in men[8]. According to a recent World Health Organization report, major depression is the leading cause of disability worldwide, with a global total of over 50 million years lived with disease in 2015[9]. The central feature of MDD is a depressive episode lasting at least two consecutive weeks. According to the DSM-5[4], five or more of the following symptoms must be present for a diagnosis of MDD, at least one of which is depressed mood or loss of interest or pleasure:

1) Depressed mood;
2) Loss of interest or pleasure;
3) Significant weight loss or weight gain or decrease or increase in appetite;
4) Insomnia or hypersomnia;
5) Psychomotor agitation or retardation;

6) Fatigue or loss of energy;
7) Feelings of worthlessness or excessive or inappropriate guilt;
8) Diminished ability to think or concentrate, or indecisiveness;
9) Recurrent thoughts of death, recurrent suicidal ideation without a specific plan, a suicide attempt or a specific plan for committing suicide[4].

1.2 The Peripheral and Central Immune Systems

The peripheral immune system is the body's first line of defense against pathogenic threats, consisting of the innate and adaptive immune systems. The innate immune system is the rapid non-specific response to pathogenic stimuli, activated through host recognition of molecular patterns associated with microbes, toxins, and injury[10]. An array of defense mechanisms are utilized by innate immunity to protect the host from pathogenic threats, including physical barriers present between host and pathogen, soluble proteins or signaling molecules expressed constitutively or released following immune activation, and various immune cells (including macrophages, monocytes, and neutrophils) that recognize and destroy invading pathogens[10]. In contrast, the slower adaptive immune system is marked by added specificity in the defense response, achieved via expression of antigen-specific receptors on the cell surfaces of T- and B-lymphocytes[10]. Following primary exposure to pathogenic stimuli, genetic re-programming of T- and B-lymphocytes mediates immunological memory by these cells, effectively yielding host immunity against the same pathogen thereafter[10].

Within the CNS, the central immune response is primarily carried out by microglia, the brain's resident innate immune cells. Under normal homeostatic conditions, these cells exhibit a

ramified phenotype that is typified by extension of their highly-motile processes into the surrounding microenvironment as a surveillance mechanism (Figure 1a). However, under various adverse conditions, microglia may adopt distinct non-ramified morphologies, including ameboid, primed, reactive, rod, and dystrophic types (Figure 1b-e). As the parenchymal macrophages of the brain, microglia transition from a ramified 'resting' state to a fully activated phagocytic ameboid phenotype in the presence of pathologic stimuli, concomitantly secreting inflammatory mediators such as cytokines and reactive oxygen species as part of the activation cascade. However, microglia can also attain partially activated states, characterized by primed and reactive morphologies. Primed microglia trigger an exaggerated inflammatory response following a second exposure to pathogenic stimuli[11]. This phenotype is characterized by thickening of microglial processes and enlargement of the cell body. Other non-ramified morphologies include rod microglia, characterized by an elongated oval-shaped soma and long processes[12], and dystrophic microglia, typified by gnarling and fragmentation of processes[13]. Perivascular macrophages (Figure 1f) express many of the same markers as microglia (including CX3CR1 and ionized calcium-binding adaptor molecule 1), but have a lineage distinct from microglia. They are located within the perivascular space and are closely-associated with cerebral vasculature[14].

The CNS has historically been construed as an 'immune privileged' site, defined by its lack of immunity-induced rejection of donor tissue grafts[15,16]. Various anatomical barriers, including the endothelial blood-brain barrier (BBB), purportedly separate the brain parenchyma and the peripheral immune system, preventing exchange of immune cells and antigens across the two domains[15]. However, recent findings, including improved understanding of lymphatic drainage

anatomy, as well as observations of peripheral immune cell extravasation into the CNS, have called the brain's 'immune privileged' status into question[15]. While research into the neuroimmune axis is in its infancy, it has quickly become apparent that the line separating the peripheral and central immune systems is not as clear-cut as previously thought.

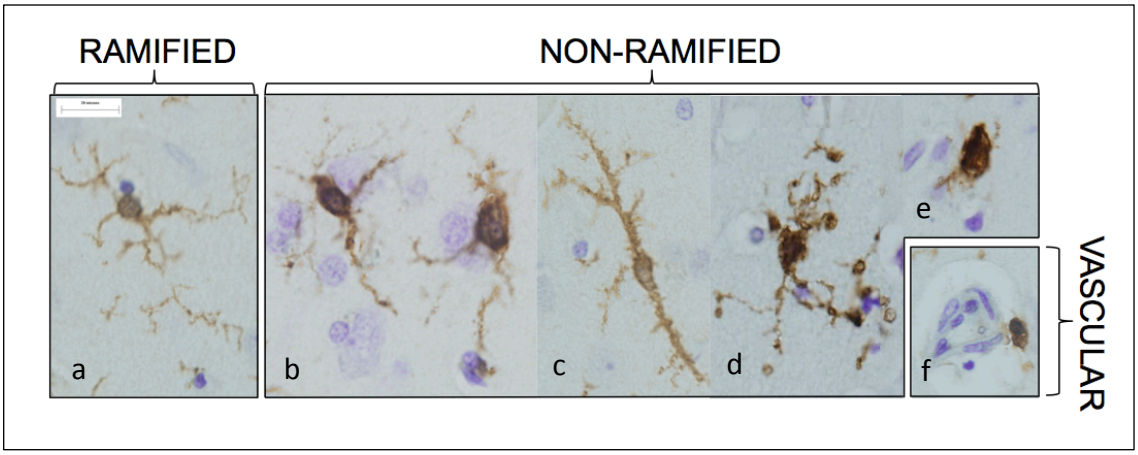

Figure 1: Photopictomicrographs of microglial morphologies.

(a-f) Examples of microglial morphologies present in the human postmortem brain of SCZ, BD, and control subjects. The following morphologies are represented: (a) ramified; (b) primed/reactive; (c) rod; (d) dystrophic; (e) ameboid; and (f) perivascular ('vascular').

1.3 Pathophysiology of Major Mental Illness

Despite decades of research, the etiology of psychiatric disorders is ill-defined, though genetic predisposition, environmental insult, and gene-environment interactions are believed to play a role. Dysregulation of structural and functional connectivity, and altered neurotransmission have been implicated as pathophysiological mechanisms[6,8,17]. Accumulating evidence from genetic and epidemiological studies, patient peripheral blood, postmortem brain tissue, and animal

models, has provided support for an immune component in neuropsychiatric conditions, including SCZ, BD, and MDD.

1.3.1 Evidence of Neuroimmune Alterations in Schizophrenia

Recent studies have shed new light on microglial functions, expanding their role from solely immune-related processes to tasks related to regulation of synaptic organization[18–20] and function[21–24], presenting a unique juncture at which immunity and brain circuitry converge. An emerging theory in SCZ research - termed the 'Microglial Hypothesis' - posits that microglial activation and altered neuron-microglia interactions underlie the connectivity alterations reported in the disorder[25].

Evidence for microglial abnormalities in SCZ comes from postmortem studies in brain and positron emission tomography (PET) imaging studies. Initial postmortem studies targeted human leukocyte antigen DR (HLA-DR) as a putative marker of microglial activation, with increased numbers of HLA-DR immunoreactive cells theoretically corresponding to an activated microglial phenotype. However, conclusions regarding HLA-DR immunoreactivity in SCZ have proven to be controversial, with some studies reporting increased HLA-DR+ microglial densities in SCZ compared to controls[26], and others finding no changes[27,28]. The specificity of HLA-DR for activated microglia has also been called into question, as reports of its expression by ramified resting cells have since surfaced[27]. In a postmortem investigation carried out previously by our lab, an antibody against ionized calcium-binding adaptor molecule 1 (IBA-1), a pan-microglial marker, was used to immunohistochemically label microglia in dorsolateral prefrontal cortex (DLPFC) from SCZ, BD, and control individuals, allowing quantification of microglial density

(cells/mm^2), IBA-1 area fraction, and microglial clustering. In white matter, we observed no changes in IBA-1 area fraction, microglial density, or microglial clustering in SCZ compared to controls[29]. Likewise, we found no changes in overall microglial density in SCZ grey matter; however, we did observe a significant decrease in IBA-1 area fraction, disturbances in morphology, and a significant increase in microglial clustering in SCZ relative to controls, suggestive of a shift in microglial function in this disorder (unpublished data).

Findings from PET imaging studies utilizing translocator protein (TSPO) as a putative marker of neuroinflammation in patient populations have been similarly mixed: while some studies reported increased TSPO availability in SCZ compared to controls[30,31], other comparable studies either found a decrease in TSPO availability in SCZ[32,33] or no differences between diagnostic groups[34,35]. Increased TSPO was initially believed to represent activation of microglia; however, it is also evidently upregulated by activated astrocytes[36], raising further questions about its interpretation in PET studies.

While altered brain cytokine levels have been described in postmortem tissue from individuals with SCZ[37–42], there has been significant disagreement in terms of which specific cytokines differ and in which direction the changes occur. For example, cortical mRNA levels of interleukin-6 (IL-6), a pro-inflammatory cytokine, were increased in the postmortem brain in SCZ in select studies[38,40], but unchanged in others[39,43], relative to non-psychiatric controls. An investigation carried out previously by our lab (which utilized the same samples as in the current study) identified no detectable changes in cortical cytokine expression levels in SCZ (unpublished data).

1.3.2 Evidence of Neuroimmune Alterations in Bipolar Disorder

Whether microglial alterations are a feature of BD is also an open question. A recent study observed decreased cortical immunostaining for the microglial markers CD68 and CD11b in BD individuals[44]. However, increased HLA-DR immunostaining was observed in patient tissue[45], while others detected no differences in microglial densities between diagnostic groups following immunostaining of brain tissue sections for IBA-1[46]. We similarly observed no changes in IBA-1 area fraction, microglial clustering, or density of microglia (cells/mm^2) in BD white matter, relative to the control group[29]. However, in grey matter, following classification of microglia according to morphological phenotype (ramified, non-ramified, or perivascular), we observed a significant reduction in the density of non-ramified microglia in the BD group relative to the control group (unpublished data), suggesting microglial activation status may be altered in the disorder. While clustering was unchanged in BD grey matter, IBA-1 area fraction was significantly reduced when compared to controls (unpublished data).

Studies quantifying expression of microglial markers at the mRNA and protein levels are also inconsistent. Increased cortical expression of CD11b mRNA and protein has been reported in the disorder[45], contradicting findings of reduced CD11b transcript levels in cingulate cortex of BD individuals[44]. Furthermore, reduced HLA-DR gene expression was identified in BD individuals using microarrays and subsequent validation through quantitative reverse transcription polymerase chain reaction (RT-PCR)[47], in disagreement with HLA-DR immunostaining results, referenced above. More recently, no evidence of altered microglial activation status was found in

BD following mRNA expression analysis of microglial and inflammatory markers in various brain regions[46].

Despite various reports of dysregulated peripheral cytokine levels in the disorder[48–50], few studies have quantified brain-resident cytokines in BD. Select analyses have indicated that postmortem frontal cortex levels of interleukin-1β (IL-1β) mRNA and protein are increased in BD relative to controls[45,51], as are cortical protein levels of IL-6 and tumor necrosis factor-α (TNFα)[51,52], though other studies found no difference in IL-6 or TNFα levels between groups[39,45]. Previously, our lab observed a significant decrease in mRNA levels of interleukin-10 (IL-10), an anti-inflammatory cytokine, in the postmortem brain of BD individuals compared to controls (unpublished data), in contrast to a prior report of increased IL-10 cortical levels[51].

1.3.3 Evidence of Neuroimmune Alterations in Major Depressive Disorder

Postmortem studies utilizing HLA-DR and quinolinic acid as markers of microglial activation have thus far failed to find an effect of MDD diagnosis. However, significant microgliosis was observed in the anterior cingulate cortex (ACC), a region implicated in depression, of individuals who died by suicide[53,54]. These observations are in agreement with a postmortem morphological investigation by Torres-Platas and colleagues, who found increased ratio of primed to ramified microglia, as well as increased density of blood vessel-associated IBA-1-positive cells, in depressed subjects who died by suicide, but no changes in depressed subjects who died of other causes. Furthermore, they detected increased mRNA expression of the immune markers IBA-1, CD45 (a marker of perivascular macrophages), MCP-1 (a factor involved in monocyte

recruitment), and ZO-1 (a factor involved in BBB permeability) in ACC white matter of depressed individuals who died by suicide[55].

While two PET imaging studies found an effect of diagnosis on cortical TSPO availability in depressed patients[56,57], most studies have found little evidence of increased neuroinflammation in MDD compared to controls[53–55,58,59]. Instead, the data suggest increased TSPO may be associated with severity of mood symptoms, with one study finding a direct correlation between ACC TSPO availability and depression severity scores, after controlling for TSPO genotype[58]. Indeed, both studies finding an effect of diagnosis on TSPO binding tended to primarily include individuals in the midst of a major depressive episode in the sample cohorts[56,57], excluding remitted and mild to moderately depressed patients.

How increased microglial activation might contribute to the pathophysiology of MDD in severely depressed and suicidal patients is currently an active area of research. Some have suggested that activated microglia may enhance excitotoxic levels of glutamate, in line with observations of increased immunoreactivity of the microglial NMDA receptor (NMDAR) agonist quinolinic acid in the MDD ACC, particularly in regions with high NMDAR density[54]. Dysregulation of the neuroimmune axis may also shift the balance of microglial and astrocytic processes in favor of a pro-inflammatory microglial phenotype, leading to hyperglutamatergia and hyposerotonergia[60]. Others have theorized that altered microglial function may suppress hippocampal neurogenesis, a mechanism believed to underlie MDD and a target of antidepressants[61].

1.4 The Fractalkine Signaling Pathway

A multitude of signaling molecules are known mediators of microglial function, including CX3CL1 (also called 'fractalkine'), CD200, CD47, various neurotransmitters, purines (ATP and UTP), MMP-3, and TREM2[62]. The abundant expression of both fractalkine and its receptor CX3CR1 in the brain[63] led to suggestions that signaling between the two fulfills an essential brain function. Recent data indicates that fractalkine, secreted by neurons, and CX3CR1, present in microglia, play a major role in neuron-microglial communication, including microglial activation and synaptic plasticity, as described below.

1.4.1 Fractalkine

CX3CL1 (fractalkine) is the sole member of the CX_3C chemokine family, consisting of a signal peptide (residues 1-24), an N-terminal chemokine domain (residues 25-100), a mucin-like stalk (residues 101-341), a transmembrane segment (residues 342-360), and a C-terminal intracellular domain (residues 361-397)[64]. Unlike most chemokines, CX3CL1 has both membrane-bound and soluble forms, with the soluble form of fractalkine produced via proteolytic cleavage by ADAM10[65], ADAM17/TACE[66,67], or cathepsin S[68,69]. Fractalkine has been well-characterized in the vascular endothelium, where it's membrane-bound form functions as an adhesion molecule and its soluble form chemoattracts CX3CR1+ monocytes, natural killer cells, and T-lymphocytes[70]. The cellular source of its expression in the brain at physiological conditions is generally attributed to neurons[24,71–73], though microglial and astrocytic expression of the chemokine has also been reported in neurodegenerative and neuroinflammatory conditions[74,75]. There is some debate as to whether fractalkine is expressed in both grey matter and white matter. Initial studies indicated fractalkine mRNA was enriched in grey matter areas at physiological

conditions, particularly in the cortex and hippocampus[72]; however, reports of its expression in white matter have since surfaced[75].

In the twenty years since human fractalkine was first identified by Bazan and colleagues[64], the *in vivo* molecular structure of the 397 amino acid protein chain is still only partially understood. While its amino acid sequence predicts a molecular weight of 42kDa[76], *O*-glycosylation of Ser and Thr residues within the mucin stalk yields a mature membrane-bound form that has been described at 65kDa[71], 90kDa[77,78], 95kDa[79], and 100kDa[66,80,81]. The soluble form has been described at 36 kDa[71], 40 kDa[71], 50-55kDa[69,71,82], 75 kDa[78], 85kDa[66,80,81], and 95kDa[64]. The inconsistencies in observed molecular weight of soluble fractalkine suggest the existence of multiple forms of the secreted chemokine, purportedly generated by cleavage at alternative sites along the mucin stalk or by other unknown mechanisms. Cleavage of fractalkine was initially predicted at a membrane-proximal dibasic motif (Thr-Arg-Arg-Gln at amino acids 338-341) due to sequence similarity with the syndecan-1 cleavage site[64,76]. However, subsequent studies have since cast doubt on the di-arginine position as the sole fractalkine cleavage site, finding that mutation of the juxtamembrane sequence failed to completely abolish shedding by metalloproteases[66,67]. Evidently, cleavage of the fractalkine ectodomain can occur at multiple sites along the mucin stalk, with inducible shedding by ADAM17/TACE occurring between amino acids 311-325[66], inducible and constitutive shedding by ADAM10 occurring at distinct membrane-proximal sites (producing 9kDa and 16kDa C-terminal fragments)[83], and shedding of a 55kDa form occurring within the first 206 amino acids of the fractalkine sequence[83] (Figure 2). The functional differences between each cleavage variant have not yet been well defined.

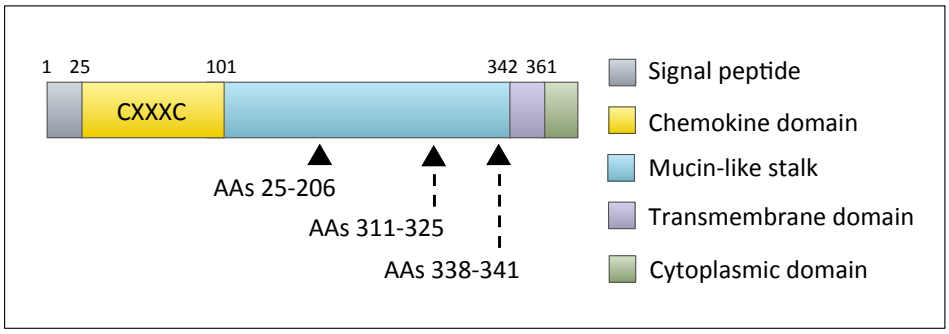

Figure 2: Diagram of immature fractalkine peptide and putative cleavage sites.

Hypothesized cleavage sites (black arrows) are proposed to exist within the first 206 amino acids (AAs), between AAs 311 and 325, and at a di-arginine site between AAs 338-341.

1.4.2 CX3CR1

Expression of the fractalkine receptor CX3CR1, a G-protein coupled receptor, is largely restricted to microglia at physiological conditions[72,84–86], with occasional reports of CX3CR1 expression by neurons and astrocytes in neurodegenerative states[24,75]. The distribution of CX3CR1 throughout the brain is controversial, with mixed findings as to whether expression is present in both grey and white matter areas or is limited to one or the other. Shortly after initial discovery of the microglial receptor, *in situ* hybridization experiments revealed uniform mRNA expression of CX3CR1 throughout the rodent brain at physiological conditions, in approximately equal quantities in grey and white matter regions[72]. However, *in situ* hybridization and immunohistochemistry for CX3CR1 has since yielded differing results, depending on the source of the tissue (human versus rodent), disease conditions, developmental timepoint, and brain region of interest[75,87].

1.4.3 Fractalkine Signaling and Microglial Activation

Despite some discrepancies in cellular and regional localization, observations of fractalkine and CX3CR1 expression by neurons and microglia, respectively, led to characterization of the pathway as a means of communication between these two cell types, with fractalkine purported to mediate migration and cell adhesion of CX3CR1-positive microglia to neuronal sites[71]. In addition, studies have characterized the pathway as a neuronal feedback mechanism for limiting microglial activation, and ultimately neurotoxicity, with mounting evidence that fractalkine downregulates microglial expression of cytotoxic mediators, including TNFα[88–90], interleukin (IL)-1β[91], and IL-6[90], as well as markers of oxidative stress[89,90]. Impact of immune challenge with the bacterial endotoxin lipopolysaccharide (LPS), including morphological transformation of microglia to the activated phenotype, is attenuated by fractalkine signaling[85,90]. Still, there is significant disagreement as to whether fractalkine signaling is neuroprotective or neurotoxic in the central nervous system (CNS)[92]: disruption of the pathway appears to have beneficial actions in certain models of Alzheimer's disease (AD) [93,94] and stroke[95,96], but damaging effects in other models of AD[97,98], amyotrophic lateral sclerosis (ALS)[85], and Parkinson's disease (PD)[85].

One explanation for these inconsistencies proposes that control of microglial activation by fractalkine signaling is context- and ligand-dependent[92]. For example, Clark and colleagues found that membrane-bound and soluble fractalkine forms produce differential pain responses in rodent models of neuropathic pain, with administration of the chemokine domain, but not full-length fractalkine, eliciting mechanical allodynia[99]. Differential effects of soluble and full-length fractalkine have also been observed in models of PD, with motor coordination deficits, neurodegeneration, and microglial activation rescued by treatment with exogenous soluble, but

not full-length, fractalkine[78]. The neuroprotective effects of fractalkine signaling may also be temporally-dependent. In a mouse model of traumatic brain injury, knock-out of the CX3CR1 gene ($CX3CR1^{KO}$) was associated with a transient reduction in learning impairment, neuronal cell death, and expression of pro-inflammatory cytokines in the first 15 days post-injury, while 30 days post-injury, $CX3CR1^{KO}$ mice exhibited increased cognitive deficits, neuronal loss, and increased cytokine expression compared to wildtype mice[100]. A separate study examined the effects of LPS on fractalkine and CX3CR1 mRNA expression in cultured rat neurons and microglia, finding that CX3CR1 transcript levels were downregulated within the first 10 hours of LPS incubation, but recovered after incubation for 24 hours[101]. Collectively, these studies indicate that fractalkine signaling is highly dynamic, with the pathway's neuroprotective or neurotoxic actions contingent upon the form of the fractalkine ligand, the context of the brain condition, and the time course of disease progression.

1.4.4 Regulation of Synaptic Density and Function by the Fractalkine Pathway

In a seminal study by Paolicelli and colleagues, microglia were demonstrated to be vital mediators of normal brain development, engulfing unnecessary synaptic elements during critical periods of postnatal development[18] in a process termed 'synaptic pruning'. Moreover, synaptic engulfment by microglia occurred in a fractalkine signaling-dependent manner: mice lacking CX3CR1 exhibited significant delays in synaptic pruning of excitatory synapses, resulting in deferred maturation of synaptic function and plasticity[18]. A subsequent study by the same research group found that a transient delay in synaptic pruning had lasting consequences on neurodevelopmental outcome, with loss of the fractalkine receptor in $CX3CR1^{KO}$ mice associated with long-term deficiencies in excitatory synapse maturation and functional brain

connectivity in adulthood[19]. Specifically, adult CX3CR1^{KO} mice exhibited lasting deficits in synaptic multiplicity, the number of synaptic contacts between a pair of neurons, as well as reductions in gross cortico-hippocampal connectivity, compared to wildtype mice[19]. More recently, a role for fractalkine-CX3CR1 interactions in microglial synaptic engulfment was reported in a mouse model of sensory lesion-induced synapse elimination[20]. In this study, whisker trimming, a paradigm known to induce synapse elimination within the rodent barrel cortex, of otherwise healthy postnatal CX3CR1^{KO} mice was followed by concomitant defects in microglial removal of thalamocortical inputs, with effects lasting beyond maturation. Taken together, these findings indicate that intact fractalkine signaling is essential for regulation of synaptic density by microglia in the uninjured developing brain, with effects persisting well into adulthood. However, whether the fractalkine-CX3CR1 axis is involved in microglial recognition of synaptic sites or whether it simply mediates proliferation of microglia throughout the brain during neurodevelopment remains to be determined. Future studies will also need to determine if perturbations in the fractalkine pathway under physiological conditions in the adult brain are similarly associated with alterations in synaptic organization, or whether this feature is specific to the developmental period.

Though poorly understood, fractalkine-CX3CR1 interactions may also have neuromodulatory effects on synaptic transmission, an attribute common to many chemokines. Unlike other chemokines, fractalkine (as well as its receptor) is abundantly expressed in the hippocampus, where it acts as a potent modulator of neuronal excitability, restricting the frequency of spontaneous glutamate release, tempering postsynaptic AMPA current amplitude, and enhancing NMDA responses[21,22,102–104]. The fractalkine pathway's capacity to manipulate synaptic activity

in hippocampal neurons may have severe consequences on hippocampal-dependent functions, including memory formation: Rogers and colleagues, for example, reported dramatic impairments in long-term potentiation, motor learning, and associative learning in $CX3CR1^{KO}$ mice[23]. Other non-hippocampal brain regions may also be substrates of fractalkine-CX3CR1 neuromodulation. In rat dorsal raphe nucleus slice preparations, application of fractalkine selectively boosted spontaneous and evoked GABA current amplitudes in serotonergic neurons, holding broad implications for serotonin-related mood disorders[24]. Enrichment of fractalkine immunoreactivity has been further observed in cortical areas, particularly in pyramidal projection neurons[105], suggesting the neuronal ligand contributes in some way to cortical function. Indeed, pyramidal neuron $GABA_A$ current was modified by treatment with exogenous fractalkine in cortical slice preparations from patients with mesial temporal lobe epilepsy[106]. However, the neuromodulatory capacity of the fractalkine-CX3CR1 axis in the cortex under normal homeostatic conditions is insufficiently understood and requires further characterization.

1.4.5 Fractalkine Signaling in Psychiatric Disorder

Given prior reports implicating CX3CR1 in severe psychiatric disorder, it is plausible that fractalkine signaling may play a role. While to date few studies have examined fractalkine signaling in these disorders, intriguingly, a recent genetic association study identified a significant association between rare sequence variants in the fractalkine receptor CX3CR1 gene and a schizophrenia phenotype[107]. Additional support for a CX3CR1 role in psychiatric disorder comes from a meta-analysis of microarray data demonstrating a significant decrease in mRNA expression in postmortem brain and blood of individuals with SCZ[108]. Furthermore, significantly reduced CX3CR1 transcript levels was observed in circulating monocytes from patients with BD

relative to controls[109]. Finally, CX3CR1-deficiency was associated with resistance to either depressive-like behavior, microglial hyper-ramification, or antidepressant treatment in a mouse model of chronic depression[110].

1.5 Research Hypotheses

Given prior reports of altered fractalkine signaling in severe psychiatric disorder, the fractalkine pathway is a promising candidate mediator of microglial dysfunction and synaptic disorganization in SCZ, BD, and MDD. However, beyond initial studies of CX3CR1 mRNA expression in brain tissue in SCZ, as described above, the protein or mRNA expression of fractalkine and molecules that cleave fractalkine, such as ADAM10, are uncharacterized in psychiatric disorder, leaving an incomplete picture of the function of this pathway. In the present study, we investigate expression of the fractalkine pathway members fractalkine, CX3CR1, and ADAM10 in the postmortem brain of SCZ, BD, MDD, and control individuals to determine the relevance of this signaling pathway to psychiatric disorder. We hypothesize the following:

1. mRNA and protein expression of fractalkine pathway members (fractalkine, CX3CR1, and ADAM10) are significantly altered in SCZ, BD, and MDD.

2. Fractalkine signaling is associated with microglial morphology in the postmortem brain of individuals with psychiatric disorder.

3. Fractalkine signaling is associated with synaptic density in the postmortem brain of individuals with psychiatric disorder.

Chapter 2: Materials and Methods

2.1 Human Tissue Samples

2.1.1 Stanley Array Series

Postmortem human brain tissue was obtained from the Array Collection at the Stanley Medical Research Institute (SMRI; Bethesda, MD, USA). The Array Collection includes biological samples from 104 subjects, including 35 with SCZ, 34 with BD, and 35 non-psychiatric controls (CON). After receiving permission from next of kin, brain tissue was collected and processed as previously described[111]. Demographic information was recorded for each subject (Table 1), including sex, age, body mass index (BMI), age of onset, total duration of hospitalizations, psychiatric diagnosis, prescribed medications, medical comorbidities, brain weight, brain hemisphere each tissue sample originated from, interval between death and refrigeration of body, and interval between death and autopsy [postmortem interval (PMI)]. Lifetime antipsychotic dose equivalent to Fluphenazine milligrams was also estimated for each individual. Data on smoking status, alcohol consumption, and use of illicit drugs was available for most, but not all, cases. Both alcohol and drug use were categorized on a scale of 0 to 5, where 0 = little or no use, 1 = social use, 2 = moderate past use, 3 = moderate present use, 4 = heavy past use, and 5 = heavy present use. Cause of death was provided, and for simplification was divided into the following categories: 'pneumonia', 'cardiac', 'accident, suicide or overdose', and 'other'. Information on levels of C-reactive protein (CRP), a measure of systemic inflammation quantified in patient blood sera by multiplex assay, was downloaded from the Brain Bank database[112]. Following acquisition of available clinical data, independent diagnosis was made by two senior psychiatrists according to criteria outlined in the Diagnostic and Statistical Manual of Mental Disorders (DSM) IV. Brain tissue samples underwent neuropathological examination to

rule out any presence of neurodegeneration or other neuroanatomical abnormalities and were further assessed for pH and RNA integrity number (RIN). All biological samples were stored at -70°C until further use.

	CON (n=35)	SCZ (n=35)	BD (n=34)
Age (years, mean, SD)	44.2 (7.6)	42.6 (8.5)	45.4 (10.7)
Sex# (male/female)	26/9	26/9	16/18
PMI (hours, mean, SD)	29.4 (12.9)	31.4 (15.5)	37.9 (18.6)*
Brain pH (mean, SD)	6.6 (0.3)	6.5 (0.2)*	6.4 (0.3)*
RIN (mean, SD)	7.2 (0.9)	7.4 (0.6)	7.3 (0.9)
Brain Hemisphere (right/left)	16/19	17/18	19/15
BMI (mean, SD)	30.9 (9.0)	31.5 (8.2)	28.9 (10.1)
Age of Onset (years, mean, SD)	N/A	21.3 (6.1)	25.3 (9.2)
Duration of Illness (years, mean, SD)	N/A	21.3 (10.2)	20.2 (9.5)
Cause of Death: Suicide# (No. of subjects)	0	7	15
Lifetime Antipsychotic Dose (mg Flu., mean, SD)	0	85,004 (100,335)	10,212 (22,871)
Prescribed Mood Stabilizers (No. of subjects)	0	11	23
Prescribed Antidepressants (No. of subjects)	0	9	19
Alcohol History# (0-1/2+)	30/5	17/18	12/21
Smoking at Death# (no/yes)	9/9	4/23	6/15
Serum CRP (mg/L, mean, SD)	13.3 (27.1)	75.4 (125.8)*	35.6 (83.4)

Table 1: Demographic and biological data for subjects in the Array Collection.

(*) indicates significance at $p<0.05$ using ANOVA with contrasts for quantitative demographic variables (not including medication values). (#) indicates significance at $p<0.05$ using Chi-squared Test for qualitative demographic variables (not including medication values).

2.1.2 Stanley Depression Series

Postmortem human brain tissue was obtained from the Depression Collection at the SMRI, which includes tissue samples from 36 subjects, including 12 cases of depression with psychosis (MDD+Psychosis), 12 cases of depression without psychosis (MDD−Psychosis), and 12 non-psychiatric controls (CON). Similar to the Array Collection, demographic information was recorded for each individual (Table 2), including sex, age, age of onset, psychiatric diagnosis, prescribed medications, cause of death, brain weight, brain hemisphere each tissue sample originated from, interval between death and refrigeration of body, and postmortem interval (PMI). Lifetime antipsychotic dose was estimated for each individual in Fluphenazine equivalents. If known for the individual, alcohol history, illicit drug use, and smoking status at time of death were also recorded. As in the Array Collection, each subject in the Depression Collection received an independent diagnosis by two senior psychiatrists according to criteria outlined in the DSM-IV. Brain tissue samples were examined by a qualified neuropathologist to exclude the possibility of neuroanatomical abnormalities and were further assessed for pH and RNA integrity number (RIN). Tissue samples were then stored at -70°C until further use.

	CON (n=12)	MDD+Psychosis (n=12)	MDD−Psychosis (n=12)
Age (years, mean, SD)	46.8 (12.1)	41.5 (12.0)	42.8 (10.1)
Sex (male/female)	8/4	6/6	7/5
PMI (hours, mean, SD)	25.2 (10.6)	35.8 (14.0)*	23.6 (6.7)
Brain pH (mean, SD)	6.64 (0.18)	6.59 (0.14)	6.71 (0.14)
RIN (mean, SD)	7.47 (0.634)	7.59 (0.738)	7.64 (0.696)
Brain Hemisphere (right/left)	6/6	4/8	5/7
Age of Onset (years, mean, SD)	N/A	29.2 (12.0)	30.6 (12.2)
Duration of Illness (years, mean, SD)	N/A	12.3 (7.0)	12.3 (8.5)
Cause of Death: Suicide# (No. of subjects)	0	9	8
Lifetime Antipsychotic Dose (mg Flu., mean, SD)	0	2,073 (2,018)	373 (921)
Prescribed Mood Stabilizers (No. of subjects)	0	2	4
Prescribed Antidepressants (No. of subjects)	0	7	10
Alcohol History (0-1/2+)	6/6	5/4	6/4
Smoking at Death (no/yes)	3/4	2/4	4/1

Table 2: Demographic and biological data for subjects in the Depression Collection.

(*) indicates significance at $p<0.05$ using ANOVA with contrasts for quantitative demographic variables (not including medication values). (#) indicates significance at $p<0.05$ using Chi-squared Test for qualitative demographic variables (not including medication values).

2.2 Immunoblotting

2.2.1 Stanley Array Series

Brain tissue derived from dorsolateral prefrontal cortex (Brodmann Area 9) was homogenized in ice-cold tris-buffered saline (TBS; 0.1M Tris base, 1.4M NaCl, pH 7.4) and total protein concentration for each sample determined using DC Protein Assay kit (BioRad, Hercules, CA,

USA). The tissue homogenates were diluted to 2μg/μL in Laemmli Sample Buffer (BioRad, Hercules, CA, USA) and frozen at -80°C until further use. Initial studies were carried out to determine the linear range of detection for each protein of interest as well as the optimal concentration for each antibody used. Samples were then loaded within the linear range of detection for each protein of interest - 10μg for fractalkine and 20μg for CX3CR1 and ADAM10 - and run in duplicate under reducing conditions on 10% polyacrylamide gels for approximately 90 minutes at 110V. Proteins were subsequently transferred to polyvinylidene fluoride (PVDF) membranes (BioRad, Hercules, CA, USA) at 0.26A for 70 minutes and stained with Memcode Reversible Protein Stain (Pierce Biotechnology, Rockford, IL, USA). After drying completely, the final blots were imaged using a LAS-3000 Image Analyzer (FujiFilm, Tokyo, Japan). To detect proteins of interest, blots were rehydrated in methanol, incubated in blocking buffer (5% skim milk powder and 0.05% Tween-20 in TBS (TBST)) for 1 hour, and left overnight in primary antibody on an orbital shaker at 4°C. The following primary antibodies were used: rabbit anti-fractalkine (Abcam #ab25088, used at 1:5,000); rabbit anti-CX3CR1 (Abcam #ab8021, used at 1:10,000); rabbit anti-ADAM10 (Abcam #ab1997, used at 1:25,000). The following day, blots were washed 5X with 0.05% TBST and incubated in HRP-conjugated goat anti-rabbit secondary antibody (Jackson ImmunoResearch Laboratories, Inc. #111-035-045, used at 1:5,000) for 2 hours. Following a final round of washes (4X with 0.05% Tween-20 in TBS and 1X with TBS), 1 mL of Western Lighting Plus-ECL enhanced chemiluminescence substrate (Perkin Elmer, Waltham, MA, USA) was applied to each blot and blots were imaged using a LAS-3000 Image Analyzer. Science Lab Image Gauge software (FujiFilm, Tokyo, Japan) was used to quantify band density in each sample. Each band of interest was normalized to the Memcode total protein

stain as well as the average band intensity per blot, and the average of the two duplicates was used as the final value for each sample.

2.3 qPCR

2.3.1 Stanley Array Series

Total RNA was prepared using brain tissue derived from orbitofrontal cortex. RNA was converted into cDNA using Transcriptor First Strand cDNA Synthesis Kit (Roche, Mannheim, Germany). Briefly, 2µg of RNA sample were combined with master mix for a final volume of 20µL. The reaction mix was then incubated for 10 minutes at 25°C, 2 hours at 37°C, and 5 minutes at 85°C. Following reverse transcription, cDNA samples were stored at -20°C until further use. PrimeTime qPCR Primers (Integrated DNA Technologies, Coralville, USA) were purchased commercially and validated through quantitative polymerase chain reaction (qPCR). The following primers were used: fractalkine (Hs.PT.58.19601997); CX3CR1 variant 1 (Hs.PT.58.4589254); CX3CR1 variant 2 (Hs.PT.58.39576631); CX3CR1 variant 3 (Hs.PT.58.360162); ADAM10 (Hs.PT.56a.38403589); and TBP (Hs.PT.39a.22214825). The primers were tested in duplicate using SYBR Green chemistry-based detection, each with two test wells containing pooled cDNA template and two negative control wells containing nuclease-free water in place of cDNA. The reaction was performed in a 96-well plate using a LightCycler 480 II (Roche, Basel, Switzerland). In each well, 10µL of 2X SYBR Green Master Mix (Life Technologies Inc., Burlington, Canada) were combined with 2µL of appropriate primers and either 8µL of (10ng) of cDNA template or 8µL of nuclease-free water. The following temperature protocol was carried out for amplification of gene products: denaturation at 95°C for 10 minutes; amplification at 40 cycles of 95°C for 15 seconds followed by 60°C for 1 minute,

with measurements taken after each cycle completion; melting curve at 95°C for 10 seconds followed by 65°C for 1 minute then raised to 97°C at a ramp rate of 0.11°C /second; and final cooling at 40°C continuously. Crossing point (Cp) values were obtained in LightCycler 480 Software 1.5.1.62 SP3 (Roche, Mannheim, Germany) and the melting curve analysis was consistent with a single reaction product for each gene. No contamination was present in the negative control wells. Primer efficiencies were established across five four-fold serial dilutions, with efficiencies between 95% to 105% and $R^2 > 0.99$.

2.3.2 Stanley Depression Series

The same qPCR validation test was carried out to validate primers for the Depression Series; please refer to previous section for detailed description.

2.4 ddPCR

2.4.1 Stanley Array Series

cDNA samples were prepared as described above. ddPCR was carried out to measure mRNA transcript levels for fractalkine, CX3CR1, and ADAM10. In each well of a ddPCR 96-well PCR plate (BioRad, Hercules, CA, USA), 10µL (12.5 ng) of cDNA template were combined with 12.5µL QX200 ddPCR EvaGreen Supermix (BioRad, Hercules, CA, USA) and 2.5 µL gene-specific PrimeTime qPCR Primers (Integrated DNA Technologies, Coralville, IA, USA) diluted in nuclease-free water. The qPCR-validated primers were used as follows: fractalkine (Hs.PT.58.19601997, used at a concentration of 50nM); CX3CR1 (Hs.PT.58.4589254, used at a concentration of 200nM); ADAM10 (Hs.PT.56a.38403589, used at a concentration of 50nM); and the reference gene TBP (Hs.PT.39a.22214825, used at a concentration of 200nM). The

fractalkine and CX3CR1 primers were duplexed in the same well, as were the ADAM10 and TBP primers. Duplicates for each cDNA sample were run on the same plate, along with two no-template controls (in which cDNA template was replaced by an equal volume of nuclease-free water) and two pooled standards consisting of equal quantities of cDNA from all study subjects. Plates were then centrifuged for 1 minute at 1,000 rcf and loaded into a QX200 AutoDG Droplet Digital PCR System (BioRad, Hercules, CA, USA) chamber for droplet generation. During droplet generation, reaction mixtures were emulsified with Automated Droplet Generation Oil for EvaGreen (BioRad, Hercules, CA, USA) and partitioned into approximately 20,000 nanoliter-sized droplets per final 20μL sample. cDNA targets were then amplified with the following thermal cycler protocol: 95°C for 5 minutes; 40 cycles of 95°C for 30 seconds followed by 59°C for 90 seconds (using a ramp rate of 2°C per second); 4°C for 5 minutes; 90°C for 5 minutes; and held at 4°C overnight. The next day, plates were loaded into a QX200 Droplet Reader (BioRad, Hercules, CA, USA) and the number of droplets containing amplified target within each sample (henceforth referred to as sample 'copy number') detected. Quantification of sample copy numbers was carried out using QuantaSoft software (BioRad, Hercules, CA, USA). Duplicate copy numbers were averaged and normalized to TBP gene expression. The coefficient of determination between normalized replicate copy numbers in the entire Array Collection was 0.982 for fractalkine, 0.943 for CX3CR1, and 0.877 for ADAM10 (Figure 14, Appendix A.1).

2.4.2 Stanley Depression Series

Total RNA was prepared from cingulate cortex and ddPCR performed as described above. Due to limited sample volume for the depression samples, and because replicate coefficients of

determination were 0.877 or greater for the Array Collection (Figure 14, Appendix A.1), only a single well was run per sample and no-template control in the Depression Collection.

2.5 Statistical Analyses

2.5.1 Stanley Array Series

Statistical analyses were carried out in R[113] using a significance level of α=0.05. Data were transformed when necessary to conform to normality as assessed by the Kolmogorov-Smirnov test. Western blot data did not require transformation, while ddPCR data were square root-transformed. Outliers were identified and subsequently removed if they exceeded 3 standard deviations from the mean. Between-group differences in mRNA and protein levels were assessed using ANCOVA, with diagnosis and sex as fixed factors and BMI, pH, PMI, and age included as covariates in all initial ANCOVA models. RIN was also included in initial ANCOVA models for ddPCR data. A final ANCOVA model including diagnosis, sex, sex by diagnosis interaction, and any additional covariates that were significant in initial models was then fit for each target of interest. Contrasts between diagnostic groups, as well as male and female groups, were subsequently viewed within the context of each ANCOVA model. Boxplots depicting between-group differences in expression levels were rendered using untransformed data.

Effects of additional possible confounders were explored individually. ANOVA was carried out to assess effects of alcohol on expression levels. Welch Two Sample t-test was carried out to compare expression levels in psychiatric patients who had a history of antidepressant or mood stabilizer use to those who did not (omitting non-psychiatric controls). Spearman correlation was used to examine a possible association between lifetime antipsychotic dose and expression levels

of fractalkine pathway members. Effects due to cause of death were explored in isolation through ANOVA. A relationship between mRNA or protein expression levels and serum CRP was explored through Spearman correlation.

Spearman correlation was used to assess relationships between members of the fractalkine pathway, measures of microglial morphology, synaptic proteins, and white matter markers. To test whether correlations between fractalkine pathway members and synaptic proteins varied significantly in strength across diagnostic groups, Spearman correlation coefficients from each diagnostic group were Fisher Z-transformed and compared using the *cocor* package[114]. To further assess whether correlations with synaptic proteins remained significant after controlling for levels of white matter proteins, a potential confounder in this analysis, Spearman partial correlation was carried out using the *ppcor* package[115]. Correlograms of corresponding Spearman correlations were rendered using the *corrplot* package[116].

2.5.2 Stanley Depression Series

Statistical analyses were carried out in R, as described above. ddPCR data were square-root transformed to conform to normality, while immunoblotting data did not require transformation. Diagnosis, sex, sex by diagnosis interaction, pH, PMI, and age were included in initial ANCOVA models, while diagnosis, sex, sex by diagnosis interaction, and any remaining variables that were significant in initial models were included in final ANCOVA models. Two models were fit for each target of interest: one in which diagnosis was categorized into three groups (MDD with psychosis, MDD without psychosis, and non-psychiatric controls) and another in which diagnosis was categorized as two groups (MDD and non-psychiatric controls).

Boxplots of protein and mRNA expression levels by diagnostic group were rendered using the untransformed data.

Effects due to use of alcohol, medications, and cause of death were assessed individually. Possible effects for alcohol and cause of death were tested using ANOVA, while effects due to antidepressants and mood stabilizers were checked using Welch Two Sample t-test. Spearman correlation was used to explore a possible relationship between lifetime antipsychotic dose and expression of fractalkine pathway members.

Chapter 3: Results

3.1 Fractalkine Pathway Protein Levels in the Stanley Array Series

3.1.1 Raw Data Observations

Immunoblotting was carried out for fractalkine, CX3CR1, and ADAM10 in the Array Series, consisting of prefrontal cortex from individuals with SCZ, BD, and non-psychiatric controls. Bands were observed at ~55kDa for fractalkine, ~50kDa for CX3CR1 and ~70kDa for ADAM10.

3.1.1.1 Fractalkine

Immunostaining of blots for fractalkine yielded a strong band at ~55kDa in grey (Figure 3a) and white matter homogenates (Figure 15a, Appendix A.2).

Currently, there is no consensus regarding the molecular weight of fractalkine in immunoblots. While a 55kDa fractalkine band has been reported in prior studies[69,71,82,83,117,118], the identity of this band is unknown. To rule out the possibility that the band is a degradation product, we ran pooled human sample side-by-side with rat cortical tissue homogenate across four conditions: tissue that was freshly dissected and snap-frozen following sacrifice of the animal; tissue that was left at room temperature for 1 hour between dissection and freezing; tissue that was left at room temperature for 2 hours between dissection and freezing; and tissue that was stored at -80°C for several years. A prominent band was resolved at ~55kDa in human and rat samples across all test conditions (Figure 15b, Appendix A.2), suggesting that the detected protein is unlikely to be a fractalkine degradation product.

Another possibility is that the observed 55kDa is a product of antibody cross-reactivity with another closely related protein. Indeed, Lucas and colleagues found that antiserum raised against a short 22 amino acid N-terminal peptide[64] detected a non-specific 70kDa band in both lysate from CD84-transfected cells as well as a recombinant human fractalkine control[119]. However, in the same study, when immunostaining was carried out with a polyclonal antibody raised against the fractalkine chemokine domain, the same region targeted by the fractalkine antibody used in the present study, no non-specific 70kDa band was visualized, suggesting that antibodies directed against the entire fractalkine chemokine domain are unlikely to cross-react with CD84. Previous studies citing the anti-fractalkine antibody used in our experiment have demonstrated its specificity through omission of the primary and secondary antibodies[120], small interfering RNA (siRNA) knock-down of fractalkine in an animal model[121], and systemic neutralization of fractalkine protein in an animal model[122]. To further validate the anti-fractalkine antibody, we carried out immunoblotting using a recombinant human fractalkine peptide corresponding to the chemokine domain (residues 25-100; Figure 15c, Appendix A.2). This test resulted in a prominent band at ~9kDa, in agreement with the expected molecular weight of the fractalkine chemokine domain. We also carried out a negative control experiment, in which a pooled sample containing homogenate from all subjects was incubated in diluent lacking the primary antibody. No immunoreactive bands were visualized following this test (Figure 15c, Appendix A.2). Collectively, these results indicate that the band detected in our samples is specific to fractalkine.

3.1.1.2 CX3CR1

Immunostaining with an antibody raised against CX3CR1 yielded a specific band at 50kDa in grey matter (Figure 3b). The size of this protein band was in agreement with prior reports of the

observed molecular weight for this target[123–126]. We did not observe a band in homogenate derived from white matter (Figure 15b, Appendix A.2).

3.1.1.3 ADAM10

Immunostaining with an antibody raised against ADAM10 yielded a specific band at 70kDa in both grey (Figure 3c) and white matter (Figure 15c, Appendix A.2). The size of this protein band was in agreement with prior reports of the observed molecular weight corresponding to the mature form of ADAM10[127–129].

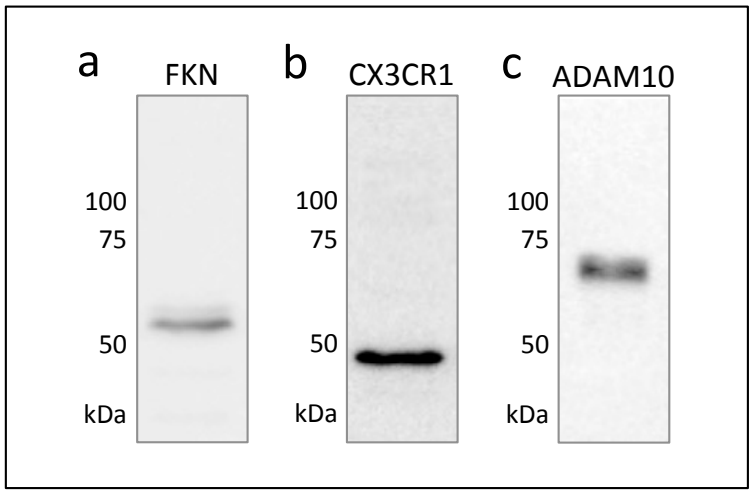

Figure 3: Immunoblotting results in Array Collection grey matter homogenates.

(a-c): Representative protein bands of a) fractalkine (FKN), b) CX3CR1, and c) ADAM10 in grey matter of Array Collection subjects within the same diagnostic group.

3.1.2 Effect of Diagnosis

Levels of fractalkine, CX3CR1 and ADAM10 were compared between diagnostic groups in the human tissue samples.

For fractalkine, we observed a significant effect of diagnosis ($F(2, 102)=4.22$, $p=.019$). When contrasts between diagnostic groups were viewed within the model context, mean fractalkine levels were reduced specifically in SCZ, compared to controls ($p=.00094$, 95% CI [-0.222, -0.058]; Figure 4a), but not in BD. We found no significant effects of pH, PMI, or age on fractalkine expression. Taken together, these findings suggest that fractalkine protein levels are diminished in SCZ relative to non-psychiatric controls.

We observed no significant effect of diagnosis on CX3CR1 levels (Figure 4b), suggesting there is no difference in mean CX3CR1 protein expression in the BD and SCZ groups relative to controls. No significant effects of PMI, pH, or age were observed for CX3CR1 protein levels.

PMI had a significant effect on ADAM10 levels ($F(1, 103)=9.40$, $p=0.003$) and was included in the final ANCOVA model. No changes in mean ADAM10 protein levels were detected across diagnostic groups after controlling for PMI (Figure 4c). No significant effects of pH or age were observed for ADAM10 protein levels.

Taken together, these observations suggest that fractalkine signaling is disrupted in SCZ, but not in BD, relative to non-psychiatric controls. No differences in protein levels were found for either the fractalkine receptor CX3CR1 or the cleavage enzyme ADAM10, indicating that disturbances in the pathway in SCZ are specific to the fractalkine ligand.

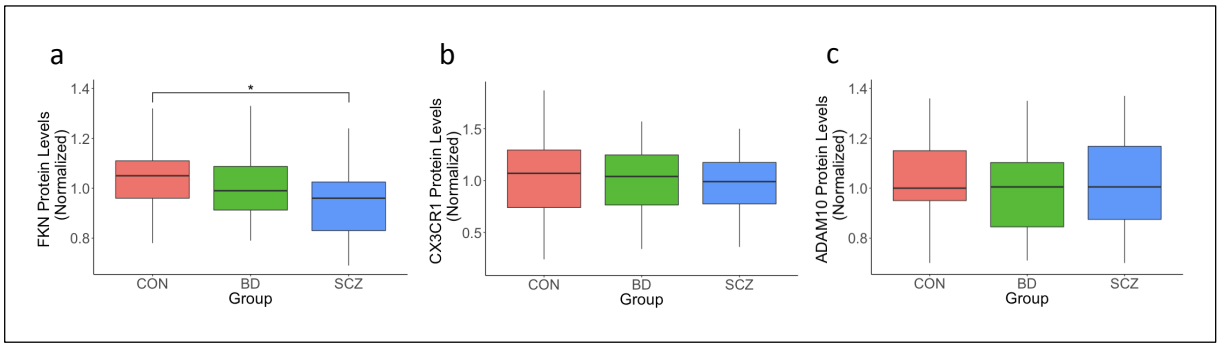

Figure 4: Effect of diagnosis on fractalkine pathway protein levels in the Array Collection.

(a-c): Normalized protein levels of (a) fractalkine (FKN), (b) CX3CR1, and (c) ADAM10 in the CON, SCZ, and BD groups quantified through immunoblotting.

3.1.3 Effect of Sex

Overall, we observed no effects of sex or sex by diagnosis interaction on fractalkine protein levels. However, closer inspection of the ANCOVA model contrasts revealed a significant effect of sex in the CON group (p=0.039, 95% CI [-0.233, -0.006]), as well as a trend towards a sex by diagnosis interaction in the SCZ group (p=0.065, 95% CI [-0.010, 0.313]; Figure 5). Collectively, these results indicate that non-psychiatric control males have higher levels of cortical fractalkine than non-psychiatric control females, with this difference not present in SCZ.

Sex had no significant effect on CX3CR1 or ADAM10 protein levels, and no sex by diagnosis interaction was observed.

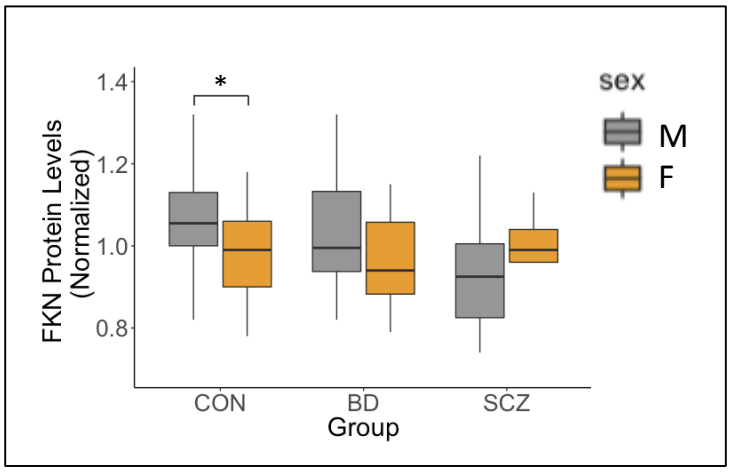

Figure 5: Effect of sex on fractalkine protein levels in the Array Collection.

A significant effect of sex on fractalkine (FKN) protein levels was observed in the CON group, but not the BD or SCZ groups.

3.1.4 Possible Confounding Variables

Possible confounders in this study include BMI, serum CRP, cause of death, substance abuse, and prescribed medications. No significant effects of BMI or serum CRP were observed for fractalkine, CX3CR1, or ADAM10 expression. Likewise, we found no significant effects of cause of death due to pneumonia, cardiac arrest, suicide, or drug overdose on protein levels. Neither alcohol nor drug use had a significant effect on levels of fractalkine pathway members. Finally, we found no evidence that use of antidepressants or mood stabilizers significantly impacted protein levels of fractalkine, CX3CR1, or ADAM10.

3.1.4.1 Effect of Lifetime Antipsychotic Dose

A significant negative association was observed between fractalkine levels and lifetime antipsychotic dose (in Fluphenazine equivalents) (Spearman ρ=-0.250; p=0.011). When groups

were examined separately, the relationship was present in SCZ (Spearman ρ=-0.391, p=0.020), but not BD (Figure 6). However, given that fewer individuals with BD were prescribed antipsychotics than those with SCZ and that lifetime doses tended to be smaller in BD than SCZ, we are unable to confidently conclude that antipsychotics have no effect on fractalkine levels in BD.

We found no evidence of a relationship between lifetime antipsychotic dose and CX3CR1 or ADAM10 protein levels.

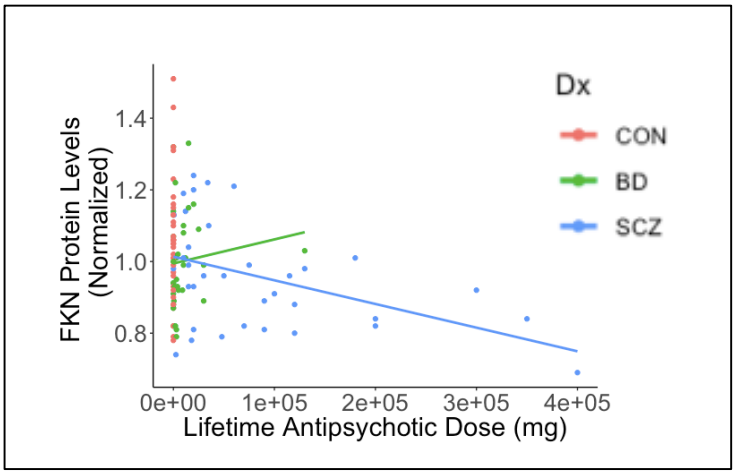

Figure 6: Plot of fractalkine protein levels and lifetime antipsychotic dose in the Array Collection.

A significant inverse relationship was observed between fractalkine (FKN) protein levels and lifetime antipsychotic dose in the SCZ, but not BD, group.

3.1.5 Correlations with Microglial Morphology and Activation Status

Past research has suggested that tonic expression and secretion of fractalkine represses activation of CX3CR1-expressing microglia[85,130,131]. To elucidate whether deficits in fractalkine signaling

are associated with abnormalities in microglial activation in SCZ or BD, we explored potential relationships between expression of fractalkine pathway members and measures of microglial morphology. Our lab previously quantified and morphologically assessed IBA-1-positive microglia present in DLPFC in a subset of the Stanley Array Series individuals[29], obtaining measures for density of the various microglial morphologies (ramified, non-ramified, and perivascular) present in our tissue.

Both fractalkine and CX3CR1 protein levels were correlated with total microglial density (fractalkine: Spearman ρ=0.35, p=0.007; CX3CR1: Spearman ρ=0.329, p=0.013; Figure 7a). CX3CR1 levels also positively correlated with density of perivascular macrophages (Spearman ρ=0.32, p=0.020; Figure 7a). We detected no significant associations between fractalkine pathway members and densities of ramified and non-ramified microglia; however, when correlations with subclasses of non-ramified microglia (categorized as primed/reactive, rod, ameboid, and dystrophic) were explored, we observed a significant relationship between fractalkine protein levels and density of primed/reactive microglia (Spearman ρ=0.326, p=0.015; Figure 7b). We also found a significant negative correlation between fractalkine protein levels and microglial clustering (Spearman ρ=-0.30, p=0.026; Figure 7c). No significant correlations were observed for protein levels of ADAM10. This is suggestive of a fractalkine signaling role in regulation of microglial distribution throughout the adult uninjured brain.

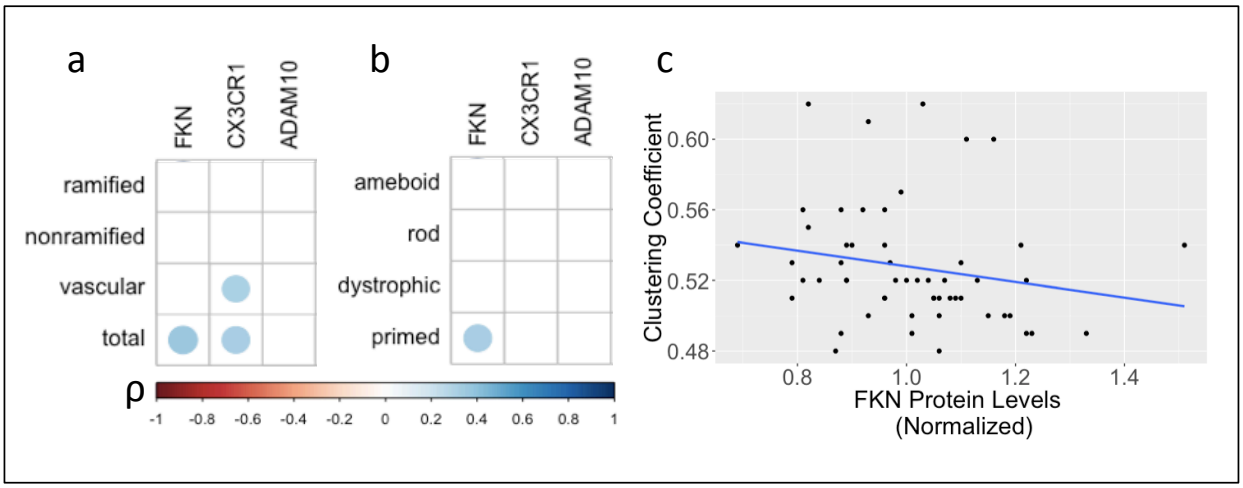

Figure 7: Correlations between fractalkine pathway proteins and microglial measures in the Array Collection.

(a) Spearman correlations between fractalkine pathway proteins and microglial densities, comprised of total microglial density and distinct morphological groups. (b) Spearman correlations between fractalkine pathway proteins and densities of non-ramified sub-groups. (c) Plot of microglial clustering coefficient by fractalkine protein levels. Only correlations significant at $p<0.05$ are represented. Abbreviations are as follows: FKN (fractalkine), primed (primed/reactive density), and vascular (perivascular macrophage density).

3.1.6 Correlations with Pre-synaptic Protein Levels

As fractalkine signaling has been implicated in mediation of synaptic connectivity in the developing and adult uninjured brain[18,132], we also examined the relationship between fractalkine and a panel of pre-synaptic proteins. Previously, our lab quantified levels of SNAP-25 in the same cohort by enzyme-linked immunosorbent assay (ELISA). SNAP-25 is a member of the SNARE complex, which facilitates exocytosis of neurotransmitter-containing vesicles from pre-synaptic terminals into the synaptic cleft[133]. Measures of additional pre-synaptic proteins, quantified in the same subjects through ELISA, were generously made available to us by Dr. William Honer, also of University of British Columbia.

Intriguingly, we observed a highly significant association between protein levels of SNAP-25 and the fractalkine receptor CX3CR1 across the entire dataset (Spearman ρ=0.56, p=6.59e-10; Figure 8a).

As SCZ and BD are believed to manifest in part from abnormal neural connectivity[17,134], this finding led us to investigate whether the association was present in all three diagnostic groups. In non-psychiatric controls, CX3CR1 levels were highly correlated with expression of SNAP-25 (Spearman ρ=0.783, p=2.71e-8; Figure 8b). In contrast, the relationship between the two proteins was substantially weakened in SCZ (Spearman ρ=0.326, p=0.056; Figure 8c) and BD (Spearman ρ=0.461, p=0.006; Figure 8d). Fisher Z-transformation[114] of correlation coefficients revealed that the strength of association between CX3CR1 and SNAP-25 differed significantly from controls in SCZ (z=2.86, p=0.002) and BD (z=2.20, p=0.014). SNAP-25 did not correlate with either fractalkine or ADAM10 across the entire dataset or within each individual diagnostic group, suggesting the relationship between fractalkine signaling and synaptic density is restricted to the fractalkine receptor.

We further examined correlations between CX3CR1 and the pre-synaptic proteins syntaxin (clone SP6), synaptobrevin (clone SP10), Septin 5 (clone SP18), complexin I (clone SP33), synaptophysin (clone EP10), synaptotagmin (clone MAb30), and complexin II (clone LP27). Protein levels of all seven pre-synaptic proteins were positively associated with CX3CR1 levels at $p<0.05$ across the entire Array Series (Figure 8a). The associations were similarly robust in the control group (Figure 8b), but severely weakened in SCZ (Figure 8c). Comparison of correlation

coefficients through Fisher Z-transformation revealed a statistically significant difference in the strength of the correlations between the control and SCZ groups for all proteins except complexin II (Table 4, Appendix B.1). While the strength of the associations was likewise decreased in BD relative to controls (Figure 8d), the difference reached statistical significance for only synaptobrevin and Septin 5 (Table 4, Appendix B.1). Though care should be taken when interpreting the relationships between levels of CX3CR1 and synaptic proteins, these findings are suggestive of a role of fractalkine signaling in the regulation of synaptic density, with potential disruptions in this function in SCZ.

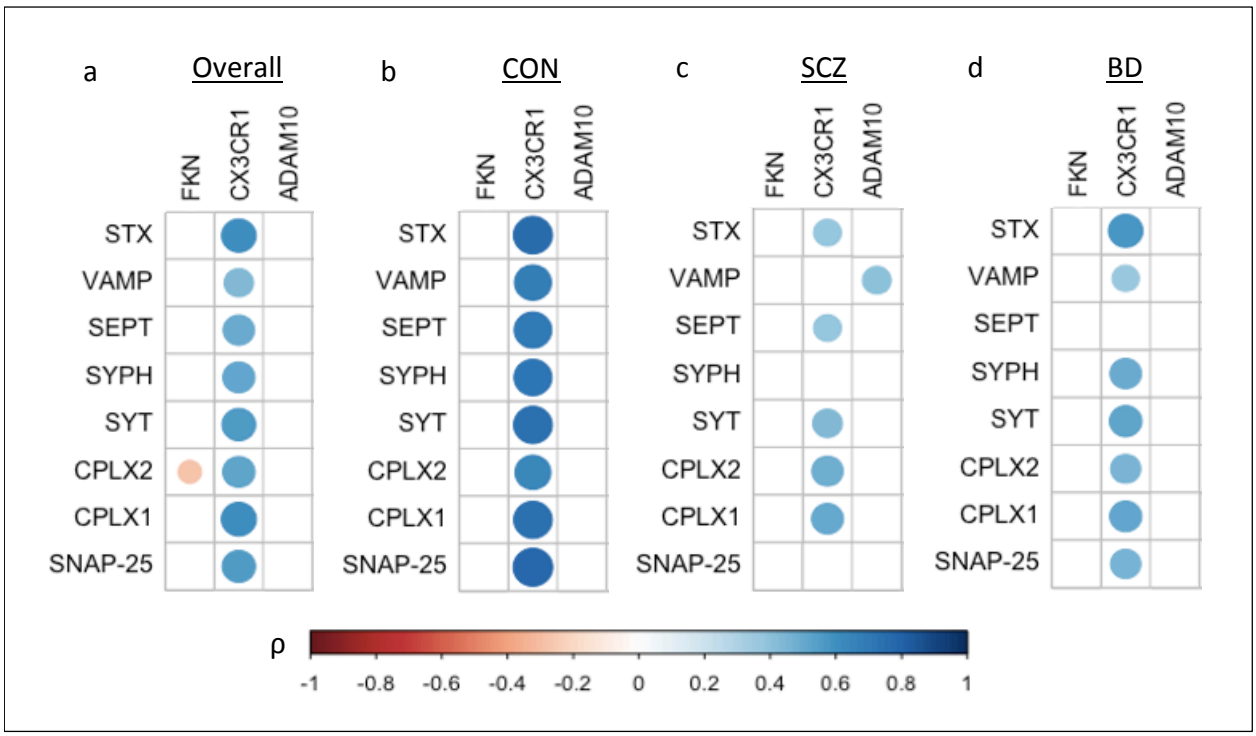

Figure 8: Correlations between fractalkine pathway proteins and pre-synaptic proteins in the Array Collection.

Spearman correlations represented across (a) the entire Array Series, (b) control subjects, (c) SCZ subjects, and (d) BD subjects. Only correlations significant at $p<0.05$ are represented. Our lab has previously quantified protein levels of SNAP-25, while measures for remaining pre-synaptic proteins were provided by W. Honer. Due to differences in immunoblotting normalization procedures, measures for syntaxin, VAMP, Septin 5, synaptophysin, synaptotagmin, complexin I, and complexin II were multiplied by (-1). Abbreviations are as follows: FKN (fractalkine); STX (syntaxin); VAMP (VAMP/synaptobrevin); SEPT (Septin 5); SYPH (synaptophysin); SYT (synaptotagmin); CPLX1 (complexin I); and CPLX2 (complexin II).

3.1.7 Correlations with Myelin-Associated Protein Levels

Given that we did not observe CX3CR1 in white matter blots, one concern regarding the significant relationship between CX3CR1 and pre-synaptic proteins is that it is an artifact of the relative proportion of grey and white matter present in each cortical homogenate. While, in

theory, each cortical homogenate should consist entirely of grey matter, there is potential for inadvertent inclusion of a small amount of white matter during the dissection process. Previously, our lab quantified protein levels of myelin basic protein (MBP), a major component of the myelin sheath that is widely used to estimate white matter content[135], in the same sample cohort using enzyme-linked immunosorbent assay (ELISA). Indeed, we found a strong negative correlation across the entire dataset between CX3CR1 and levels of MBP (Spearman ρ=-0.53, p=7.15e-9).

To address this potential confound, we carried out Spearman partial correlation, a method for measuring the association between two variables while adjusting for a third variable[115]. We re-examined the correlations between CX3CR1 and pre-synaptic proteins, this time holding levels of MBP constant. After controlling for MBP levels, CX3CR1 remained highly correlated with SNAP-25 levels (Spearman $\rho_{partial}$=0.436, p=4.15e-6), as well as levels of all other investigated pre-synaptic proteins (Table 5, Appendix B.2), across the entire Stanley Array Series. Furthermore, CX3CR1 levels remained significantly correlated with SNAP-25 expression in the control group (Spearman $\rho_{partial}$=0.702, p=3.78e-6), as well as with levels of remaining pre-synaptic proteins (Table 5, Appendix B.2), after controlling for levels of MBP. In contrast, the strength of association between CX3CR1 and SNAP-25 remained weakened in the SCZ group (Spearman $\rho_{partial}$=0.161, p=0.364), as did associations with all remaining pre-synaptic proteins, except complexin I (Table 5, Appendix B.2). The strength of the correlations between CX3CR1 and SNAP-25 (p=0.044, Spearman $\rho_{partial}$=0.353), and all pre-synaptic proteins except syntaxin (Table 5, Appendix B.2), also remained substantially weakened in the BD group. These findings suggest that despite potential inadvertent inclusion of white matter in some samples, levels of the

fractalkine receptor are closely associated with those of pre-synaptic proteins in the non-psychiatric control brain, lending additional support to a fractalkine signaling role in homeostatic regulation of synaptic density.

3.2 Fractalkine Pathway mRNA Levels in the Stanley Array Series

3.2.1 Raw Data Observations

Droplet digital PCR was carried out for fractalkine, CX3CR1, and ADAM10 in the Array Series, consisting of frontal cortex from individuals with SCZ, BD, and non-psychiatric controls. Pre-validated primers for fractalkine, CX3CR1, and ADAM10 were purchased commercially and further validated in our hands by qPCR (see Table 3 for a list of primer pairs used in the present study). Four transcript variants have been identified for the CX3CR1 gene, with variant 1 encoding the longer canonical isoform (a) and variants 2-4 encoding a shorter isoform (b)[136] (Figure 9). We tested primers against CX3CR1 variants 1, 2 and 3, ultimately opting to use the primer pair for transcript variant 1, corresponding to isoform a, because it yielded the highest qPCR reaction efficiency, with a Cp value of 28 (compared to Cp values of 30 and 34 for primer pairs against variants 2 and 3, respectively). In contrast, the primer pairs chosen for fractalkine and ADAM10 enabled simultaneous detection of all known transcript variants, resulting in Cp values of 24.5 for both genes.

Target	Primer Sequences	Assay Code
fractalkine	Primer 1: TGC CTG GTT CTG TTG ATA GTG Primer 2: CTT CTG CCA TCT GAC TGT CC	Hs.PT.58.19601997
CX3CR1 (variant 1)	Primer 1: GCC TCA GCC AAA TCA TCG TA Primer 2: GGC AGA CTT GGA TTT CAG GA	Hs.PT.58.4589255
CX3CR1 (variant 2)	Primer 1: GAA CAC AGT CCC AAA GAC CA Primer 2: TGT CCT CGG AAC ACC ACA	Hs.PT.58.39576631
CX3CR1 (variant 3)	Primer 1: GGG AAC TGA TCC ATG GTA A Primer 2:TGG GCA GGG AAG CTG AG	Hs.PT.58.360162
ADAM10	Primer 1: CAG TTA GCG TCT CAT GTG TCC Primer 2: GTA GTA ATC CAA AGT TGC CTC CT	Hs.PT.56a.38403589
TBP	Primer 1: CAA GAA CTT AGC TGG AAA ACC C Primer 2: GAT AAG AGA GCC ACG AAC CAC	Hs.PT.39a.22214825

Table 3: List of qPCR primers used in the present study.

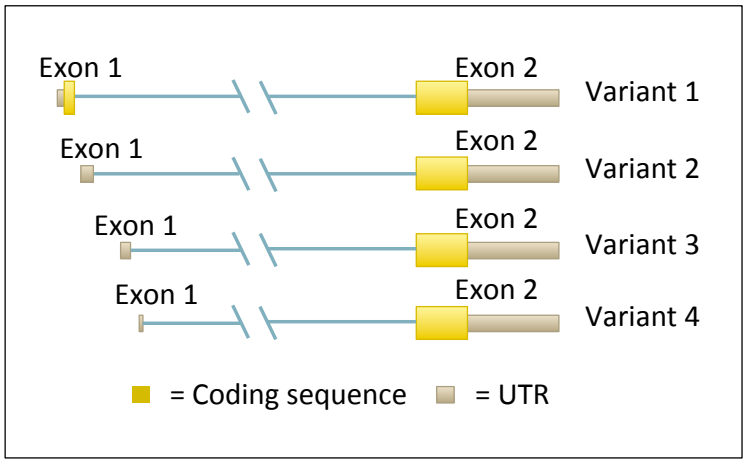

Figure 9: Diagram of CX3CR1 transcript variants.

CX3CR1 possesses four mRNA transcript variants. While primers were tested against all four, ultimately we measured levels of variant 1 in our subjects. Variant 1 encodes a longer canonical isoform of CX3CR1, while variants 2-4 encode a shorter CX3CR1 isoform. Variants 2-4 differ in their 5' untranslated region (UTR).

To quantify mRNA transcript levels of fractalkine, CX3CR1, and ADAM10, we carried out ddPCR[137,138]. Analogous to qPCR, ddPCR amplifies an RNA target sequence through the use of pre-validated primers or probes specific to the gene of interest, though with a few distinctions. First, prior to amplification, the ddPCR reaction mixture is partitioned into approximately 20,000 oil-based droplets containing varying levels of RNA template, allowing for thousands of individual PCR reactions within a single sample. Second, the ddPCR reaction is run to completion, in contrast to qPCR, in which measurements are taken after the completion of each temperature cycle. The number of droplets containing amplified product are then quantified as the final ddPCR outcome. These features allow for precise and absolute quantification of mRNA, independent of reaction efficiency and without the use of standard curves, making it advantageous for low-abundance targets such as cytokines[137–139]. Though normalization to a reference gene is not mandatory in ddPCR, we opted to normalize to TBP. In ddPCR, the separation of positive from negative droplets is based on the fluorescent signal emitted following binding of EvaGreen dye to amplified DNA product, resulting in distinct droplet clusters at corresponding amplitudes and allowing for multiplexing of PCR reactions within the same well (Figure 16, Appendix A.3). To take advantage of this feature, initial tests were carried out to optimize primer efficiency and maximize droplet separation in duplexed assays. From these results, we chose to duplex primers for fractalkine with CX3CR1, as well as ADAM10 with the housekeeping gene TBP, for all ddPCR experiments.

3.2.1.1 Fractalkine

ddPCR for fractalkine yielded an average of 171.8 copies per μL for the entire Stanley Array Series. An average of 19,544.3 (±1,280.9) droplets were generated per sample, each

approximately 1nL in volume. At least 10,000 total droplets were observed for each sample replicate. No sample replicates exhibited fewer than 5 positive droplets, the minimum droplet number recommended for accurate copy number detection[140].

3.2.1.2 CX3CR1

ddPCR for CX3CR1 yielded an average of 4.1 copies per μL for the entire cohort, with an average of 19,544.3 (±1,280.9) droplets per sample replicate, each approximately 1nL in volume. No sample replicates exhibited less than 10,000 total droplets. However, as a quality control measure, a small number of replicates exhibiting fewer than 5 positive droplets were omitted from the dataset[140].

3.2.1.3 ADAM10

ddPCR for ADAM10 resulted in an average of 37.8 copies per μL for the entire cohort. An average of 19,435.5 (±1,033.5) droplets were generated per sample replicate, each approximately 1nL in volume. At least 10,000 total droplets were observed for each sample replicate and no sample replicates exhibited fewer than 5 positive droplets.

3.2.2 Effect of Diagnosis

Fractalkine, CX3CR1 and ADAM10 mRNA levels were compared between diagnostic groups in our human tissue samples. RIN was found to have a significant effect on fractalkine mRNA expression ($F(1,103)=8.49$, $p=0.004$) and was included with sex and sex by diagnosis interaction in the final ANCOVA model. No differences in fractalkine mRNA expression between diagnostic groups were observed including diagnosis, sex, sex by diagnosis interaction, and RIN

in the model (Figure 10a). Neither pH, PMI, nor age had a significant effect on fractalkine expression.

Similarly, no significant differences in CX3CR1 mRNA expression were observed between groups, including diagnosis, sex and sex by diagnosis interaction in the model (Figure 10b). CX3CR1 transcript levels did not appear to be sensitive to effects of RIN, pH, PMI, or age.

ADAM10 mRNA levels were found to be significantly impacted by pH ($F(1,103)=15.3$, $p=1.79e-04$) and RIN ($F(1,103)=18.1$, $p=4.99e-05$); thus, pH and RIN were included in the final ADAM10 ANCOVA model. No differences in ADAM10 mRNA levels were observed between diagnostic groups, including diagnosis, sex, sex by diagnosis interaction, pH, and RIN in the model (Figure 10c). We observed no effects of PMI or age on ADAM10 mRNA expression.

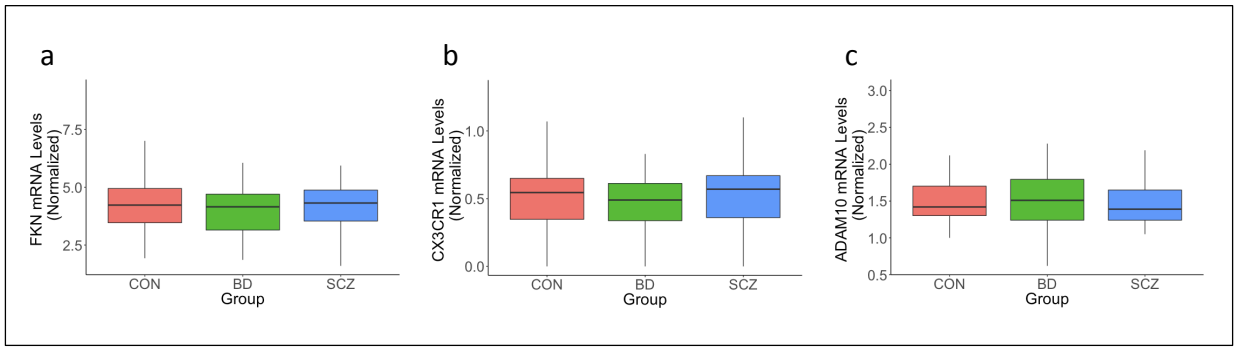

Figure 10: Effect of diagnosis on fractalkine pathway mRNA levels in the Array Collection.

(a-c): mRNA transcript levels of fractalkine (FKN), CX3CR1, and ADAM10 in the CON, SCZ, and BD groups.

3.2.3 Effect of Sex

Sex had no significant effects on mRNA expression of fractalkine, CX3CR1, or ADAM10, while no sex by diagnosis interaction was observed.

3.2.4 Possible Confounding Variables

BMI, serum CRP, cause of death, substance abuse, and prescribed medications were explored as possible confounders in our analysis of mRNA expression. We observed no effect of BMI or serum CRP levels on fractalkine, CX3CR1, or ADAM10 mRNA levels. Cause of death related to pneumonia, cardiac arrest, suicide, or drug overdose had no effect on mRNA levels, nor did either alcohol nor drugs. Finally, we found no effects of prescribed medications, including antidepressants, mood stabilizers, and lifetime antipsychotic dose, on mRNA expression of fractalkine pathway members.

3.2.5 Correlations with Microglial Morphology and Activation Status

Following quantification of transcript levels, we observed a significant positive correlation between expression of CX3CR1 mRNA and ramified microglial density (Spearman ρ=0.290, p=0.039; Figure 11a). CX3CR1 mRNA also positively correlated with total microglial density (Spearman ρ=0.274, p=0.047; Figure 11a), in agreement with a similar association observed for CX3CR1 protein levels, discussed above. In contrast, we failed to observe any association between expression of fractalkine and measures of microglial morphology. However, ADAM10 mRNA levels were negatively correlated with density of perivascular macrophages (Spearman ρ=-0.317, p=0.024; Figure 11a). Neither fractalkine, CX3CR1, or ADAM10 transcript levels correlated with subgroups of non-ramified microglia (Figure 11b). Finally, because we observed

a significant inverse relationship between fractalkine protein expression and microglial clustering, we examined a similar potential correlation with fractalkine mRNA levels. Fractalkine mRNA levels were not significantly correlated with microglial clustering coefficient in the Array series subjects (Spearman ρ=-0.083, p=0.562; Figure 11c).

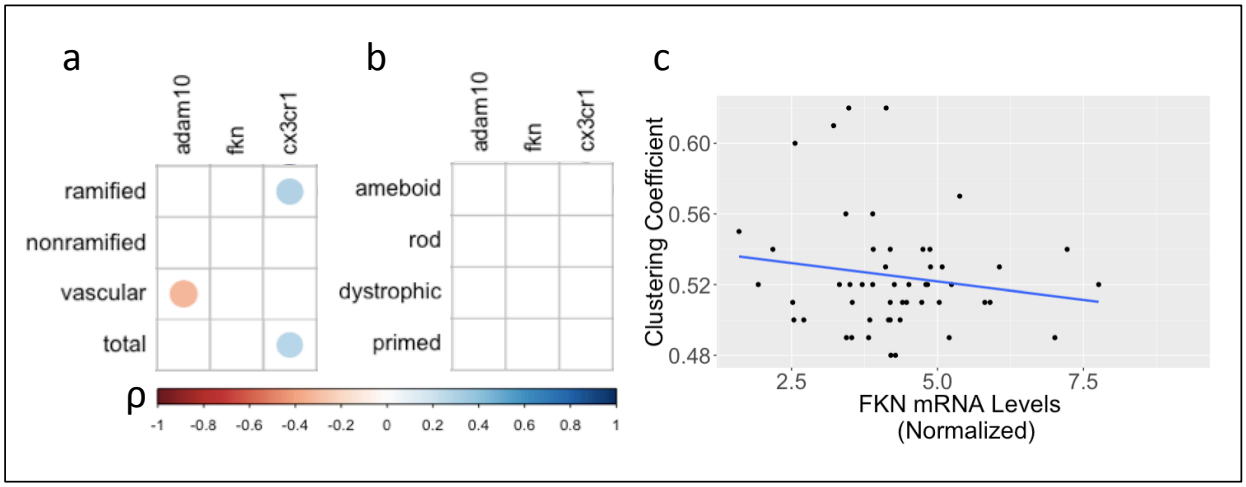

Figure 11: Correlations between fractalkine pathway mRNA levels and microglial measures in the Array Collection.

(a) Spearman correlations between fractalkine, CX3CR1, and ADAM10 mRNA levels and microglial densities, comprised of total density and densities of distinct morphological groups. Only correlations significant at $p<0.05$ are represented. (b) No Spearman correlations between fractalkine, CX3CR1, and ADAM10 mRNA levels and densities of non-ramified sub-groups were significant at $p<0.05$. (c) Plot of microglial clustering coefficient by fractalkine mRNA levels. No significant association was found between these two variables. Abbreviations are as follows: FKN (fractalkine), primed (primed/reactive density), and vascular (perivascular macrophage density).

3.2.6 Correlations with Pre-Synaptic Protein Levels

As discussed in Chapter 3.1, we detected a strong association between CX3CR1 and pre-synaptic protein levels in the postmortem DLPFC of non-psychiatric individuals. The strength of this

association appeared to be significantly reduced in SCZ. To further elucidate the link between fractalkine signaling and synaptic density, as well as potential disruptions in SCZ, we examined prospective correlations between pre-synaptic protein levels and mRNA expression of fractalkine pathway members.

CX3CR1 mRNA levels were positively correlated with protein levels of syntaxin (Spearman ρ=0.344, p=0.046), VAMP (Spearman ρ=0.358, p=0.046), and Septin 5 (Spearman ρ=0.350, p=0.043) in controls (Figure 12b), but not in SCZ (Figure 12c) or BD (Figure 12d). Comparison of correlation coefficients revealed a statistically significant difference in the strength of the correlations with VAMP (z=2.07, p=0.019) and syntaxin (z=2.56, p=0.005) in BD, but not SCZ, compared to controls. However, the difference in strength of correlation with Septin 5 was not significant in either BD or SCZ relative to the control group.

Intriguingly, fractalkine mRNA levels negatively associated with protein levels of syntaxin (clone SP6; Spearman ρ=-0.266, p=0.008) and synaptotagmin (MAb30; Spearman ρ=-0.265, p=0.008) across the entire Stanley Array Series (Figure 12a). However, when examined separately within each diagnostic group, the correlations were significant at $p<0.05$ in the SCZ (Figure 12c) and BD (Figure 12d) groups, but not in non-psychiatric controls (Figure 12b). Fisher Z-transformation and subsequent comparison of Spearman correlation coefficients revealed significant differences in the strength of the correlations with syntaxin (z=2.15, p=0.016) and synaptotagmin (z=1.68, p=0.047) in SCZ, but not BD, compared to controls.

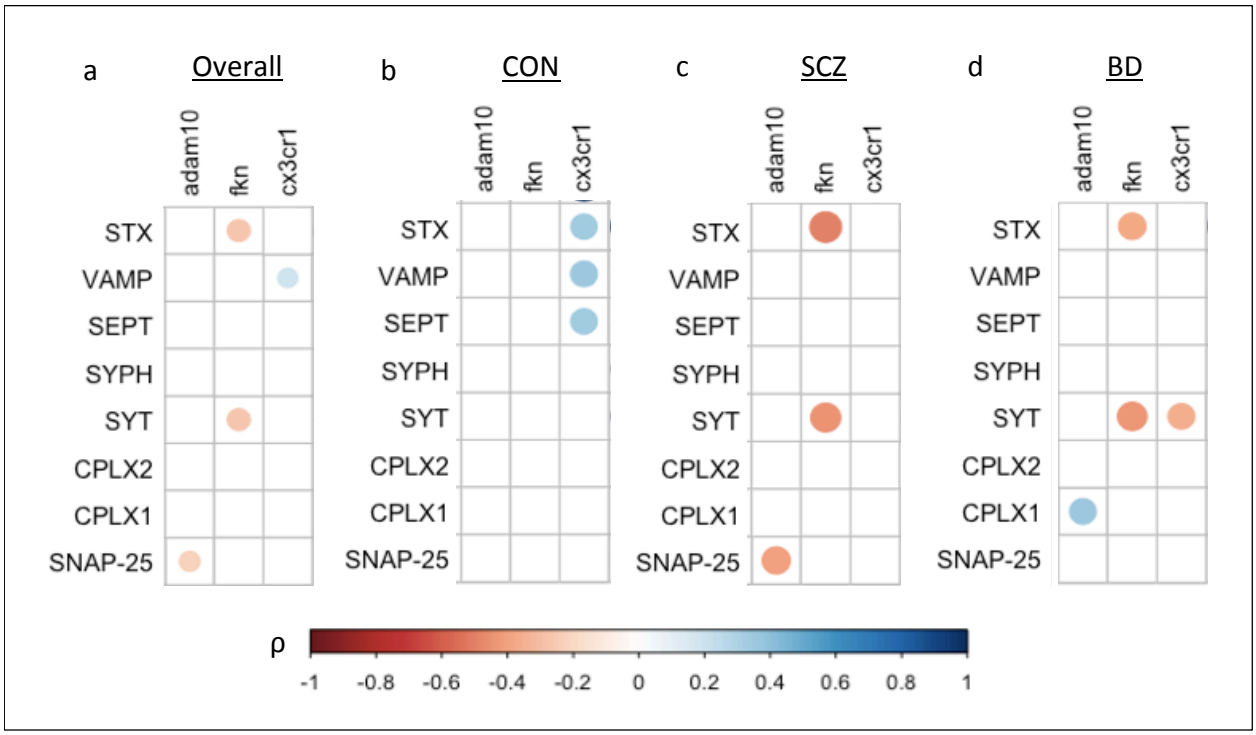

Figure 12: Correlations between fractalkine pathway mRNA and pre-synaptic proteins in the Array Collection.

Spearman correlations represented across (a) the entire Array Series, (b) control subjects, (c) SCZ subjects, and (d) BD subjects. Capitalized labels correspond to proteins levels, while lowercase labels correspond to mRNA levels. Only correlations significant at $p<0.05$ are represented. Our lab previously quantified protein levels of SNAP-25, while measures for remaining pre-synaptic proteins were provided by W. Honer. Due to differences in immunoblotting normalization procedures, measures for syntaxin, VAMP, Septin 5, synaptophysin, synaptotagmin, complexin I, and complexin II were multiplied by (-1). Abbreviations are as follows: FKN (fractalkine); STX (syntaxin); VAMP (VAMP/synaptobrevin); SEPT (Septin 5); SYPH (synaptophysin); SYT (synaptotagmin); CPLX1 (complexin I); and CPLX2 (complexin II).

Finally, a significant negative association between ADAM10 mRNA and SNAP-25 protein levels was observed in the SCZ group (Spearman ρ=-0.397, p=0.022), but not in other groups or

across the entire cohort (Figure 12c). However, the difference in strength of this correlation in SCZ did not reach statistical significance when compared to controls.

These findings provide evidence of a relation between fractalkine signaling and regulation of synaptic density and suggest that alterations in this pathway may be a feature of SCZ.

3.3 Fractalkine Pathway mRNA Levels in the Stanley Depression

3.3.1 Raw Data Observations

Droplet digital PCR was carried out for fractalkine, CX3CR1, and ADAM10 in the Depression Series, consisting of cingulate cortex from individuals with MDD and non-psychiatric controls. Primers were validated as described in Chapter 3.2. Fractalkine, CX3CR1, and ADAM10 mRNA levels were measured in the Stanley Depression Series through ddPCR. Initial tests were carried out to confirm ddPCR parameters used in the Array series, including the amount of cDNA sample, duplexing of primers in the same well (fractalkine with CX3CR1 and ADAM10 with TBP), and thermal cycler temperature protocol, were also optimal in the Depression Series using a pooled sample consisting of cDNA from all 36 subjects. Due to limited sample availability, only one replicate per sample was run. All final values were normalized to TBP expression.

3.3.1.1 Fractalkine

ddPCR for fractalkine revealed an average of 238.4 copies per μL over the entire Stanley Depression Series. An average of 18,446.3 (±1,528.5) droplets were generated per sample, each approximately 1nL in volume. Each sample yielded at least 10,000 total droplets and more than 5 positive droplets.

3.3.1.2 CX3CR1

ddPCR returned an average of 16.7 copies per µL of CX3CR1 for the entire cohort. On average, 18,446.3 (±1,528.5) droplets were generated per sample, each approximately 1nL in volume. No samples exhibited less than 10,000 total droplets. Three samples returned less than 5 positive droplets. However, due to the small sample size of this cohort, we opted to include these samples in the final analysis.

3.3.1.3 ADAM10

ddPCR for ADAM10 generated an average of 187.3 copies per µL for the entire cohort. An average of 18,741.9 (±1,239.4) droplets were generated per sample replicate, each approximately 1nL in volume. At least 10,000 total droplets and 5 positive droplets were observed for each sample.

3.3.2 Effect of Diagnosis

mRNA levels of fractalkine, CX3CR1 and ADAM10 were compared across diagnostic groups. We observed a significant effect of PMI on fractalkine mRNA expression ($F(1,103)=4.49$, $p=0.042$) when MDD and non-psychiatric control groups were compared to one another; thus, PMI was included in the final ANCOVA model with diagnosis, sex and sex by diagnosis interaction. No differences in fractalkine mRNA expression were observed between the MDD and control groups (Figure 13a). When the MDD group was further divided into MDD with psychosis and MDD without psychosis and subsequently compared to controls, we observed a trend towards an effect of PMI on fractalkine expression ($F(1,103)=3.53$, $p=0.070$) and included

it in the final ANCOVA model. No differences in mean fractalkine mRNA expression were detected across the MDD with psychosis, MDD without psychosis, and control groups (Figure 13d). RIN, pH, and age had no significant effect on fractalkine transcript levels in either analysis.

When comparing the MDD and non-psychiatric control groups, pH was found to have a significant effect on CX3CR1 transcript levels ($F(1,103)=5.95$, $p=0.021$) and was included in the final ANCOVA model with diagnosis, sex and sex by diagnosis interaction. In this analysis, there was no significant effect of diagnosis on CX3CR1 expression (Figure 13b). When the MDD with psychosis, MDD without psychosis, and control groups were compared, pH was similarly found to significantly influence CX3CR1 mRNA expression ($F(1,103)=5.50$, $p=0.026$) and was likewise included in the final ANCOVA model. In this analysis, there was still no effect of diagnosis on CX3CR1 mRNA levels (p=0.588; Figure 13e). No significant effect of RIN, PMI, or age was observed on CX3CR1 expression in either analysis.

When the MDD group was compared to controls ADAM10 mRNA levels were significantly impacted by pH ($F(1,103)=22.3$, $p=4.71e-05$); thus, pH was included in the final ADAM10 ANCOVA model in the two-group analysis. No differences in ADAM10 mRNA levels were observed between the MDD and control groups when including diagnosis, sex, sex by diagnosis interaction, and pH in the model (Figure 13c). When the MDD with psychosis, MDD without psychosis, and control groups were compared, pH was found to similarly have an effect on ADAM10 expression ($F(1,103)=21.3$, $p=7.28e-5$). No effect of diagnosis was observed on ADAM10 transcript levels in this analysis (Figure 13f). We observed no effects of RIN, PMI, or age on ADAM10 mRNA expression in either analysis.

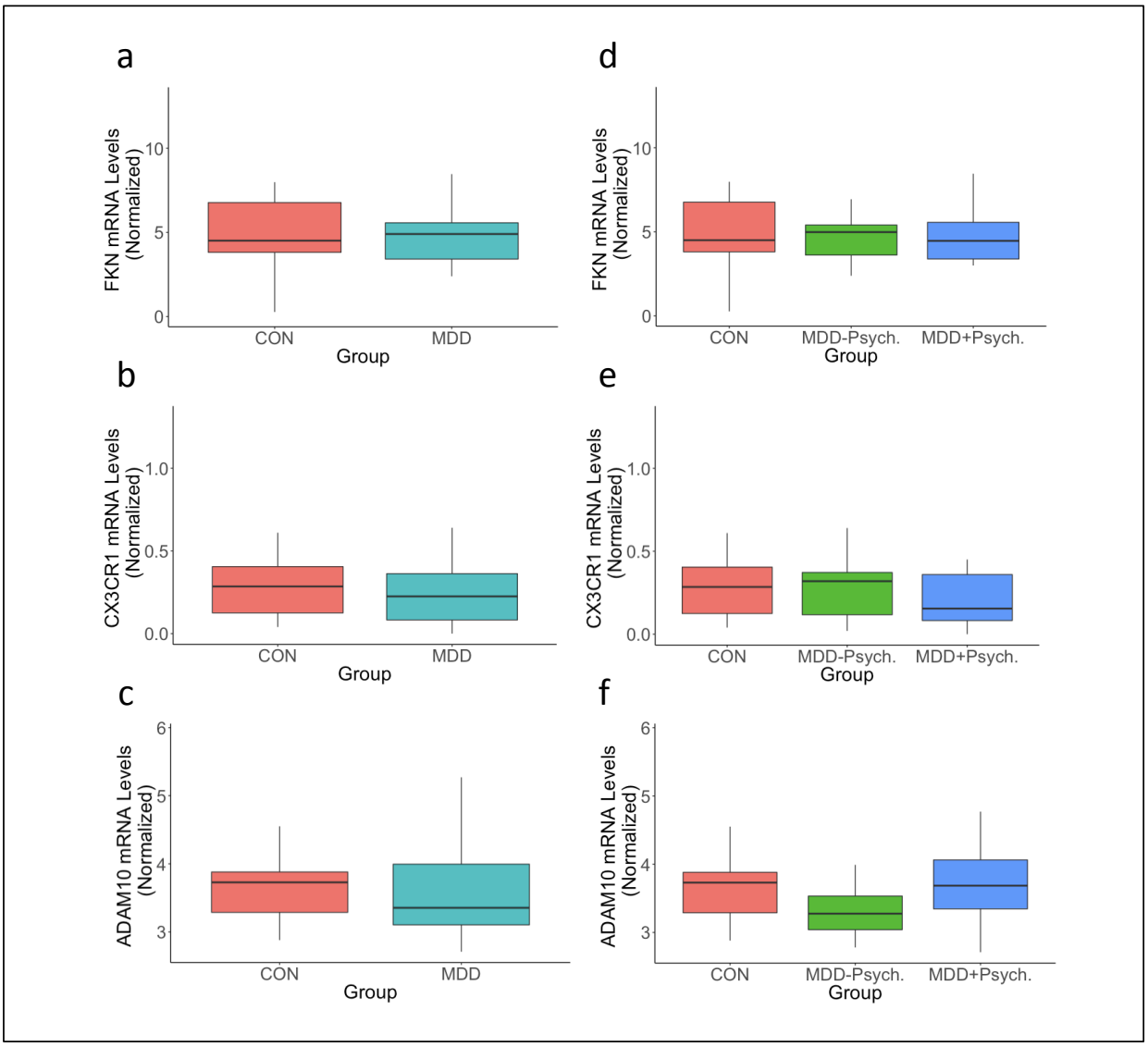

Figure 13: Effect of diagnosis on fractalkine pathway mRNA levels in the Depression Collection.

(a-c): mRNA levels of (a) fractalkine (FKN), (b) CX3CR1, and (c) ADAM10 in the MDD and CON groups. (d-f): mRNA levels of (d) fractalkine, (e) CX3CR1, and (f) ADAM10 in the MDD with psychosis, MDD without psychosis, and CON groups. No significant effect of diagnosis was observed in either analysis.

3.3.3 Effect of Sex

Sex had no significant effect on mRNA expression of fractalkine, CX3CR1, or ADAM10 and no sex by diagnosis interaction was observed.

3.3.4 Possible Confounding Variables

Cause of death, alcohol, and prescribed medications were explored as possible confounders in our analysis of mRNA expression. Cause of death related to cardiac conditions or suicide had no effect on mRNA levels, nor did alcohol use. We observed no significant effects of prescribed medications, including antidepressants, mood stabilizers, and lifetime antipsychotic dose, on transcript levels of fractalkine, CX3CR1, or ADAM10.

Chapter 4: Conclusion

4.1 Discussion

Immune disturbances have been reported in severe psychiatric disorders. Given the known functions of the fractalkine signaling pathway, this pathway is a promising candidate mediator of microglial dysfunction, and potentially also downstream synaptic disorganization, in SCZ, BD, and MDD. However, to date, little is known about the role of fractalkine signaling in these disorders. A meta-analysis of microarray data demonstrated a significant decrease in CX3CR1 mRNA expression in postmortem brain and blood in individuals with SCZ[108], with CX3CR1 expression in blood correlated with the depression-anxiety dimension of the PANSS[108]. Furthermore, a significant genetic association was reported between the CX3CR1-Ala55Thr variant and SCZ, with this mutation shown to inhibit fractalkine signalling[107]. Cortical mRNA expression of fractalkine and ADAM10, which cleaves fractalkine, as well as cortical levels of corresponding proteins, are uncharacterized in psychiatric disorder, leaving an incomplete picture of the function of this pathway. To our knowledge, this is the first study to concurrently quantify mRNA and protein levels of fractalkine, CX3CR1, and ADAM10 in grey matter of SCZ and BD subjects, as well as the first to measure fractalkine pathway transcript levels in grey matter of MDD subjects.

4.1.1 Fractalkine Protein Levels are Diminished in SCZ

We initially hypothesized that the fractalkine-CX3CR1 pathway is altered in SCZ, BD, and MDD. Here we provide evidence of fractalkine signaling dysregulation in SCZ. In particular, we observed a significant decrease in mean fractalkine protein levels in SCZ relative to non-psychiatric controls.

While the expected molecular weight of membrane bound fractalkine is around 95kDa after glycosylation, with the soluble form around 80kDa, in our hands immunostaining yielded a strong band at ~55kDa in grey and white matter homogenates. This 55kDa fractalkine band has been observed in a number of prior studies[69,71,82,83,117,118], with some suggesting it reflects an alternative cleavage product. In the brain, Pan and colleagues observed multiple splice variants of fractalkine mRNA, postulating that some may lead to truncated forms of the soluble protein[74]. Hundhausen and colleagues observed inducible expression of a 55kDa soluble fractalkine form following deletion of putative ADAM10 juxtamembrane cleavage sites[83], while Fonović and colleagues identified a 55kDa fractalkine product generated through cathepsin S cleavage[69]. Other possible explanations for the 55kDa fractalkine band include varying degrees of *O*-glycosylation of the mucin stalk; degradation of fractalkine products containing the chemokine domain[119]; and detection of fractalkine precursor protein rather than the mature, heavily glycosylated form[66,80]. We suggest that the band detected most likely represents a truncated soluble form, such as the form observed following cathepsin S proteolysis[69]. Nevertheless, further testing is needed to verify the identity of the observed 55kDa fractalkine form and the regulatory mechanisms mediating changes in SCZ.

We did not find evidence for altered fractalkine protein levels in BD. Furthermore, we did not observe any significant differences in fractalkine mRNA levels in SCZ, or in BD or MDD subjects. Others have suggested that regulation of fractalkine occurs at the protein-level in order to meet the temporal constraints demanded by a rapid inflammatory response[141]. Indeed, fractalkine is constitutively endocytosed as a means of preventing its cleavage by cell-surface

metalloproteases and stored intracellularly as a pool of precursor protein, where it can be rapidly shuttled to the membrane as needed[141]. Neither protein nor mRNA expression of CX3CR1 and ADAM10, a metalloproteinase that cleaves fractalkine into its soluble form, were altered in any disorder, indicating that disruptions in fractalkine signaling are limited to regulation of fractalkine protein in SCZ. These findings are not in agreement with a previous meta-analysis that observed decreased CX3CR1 in brain and blood of SCZ individuals[108]. Given the sample size of the meta-analysis was substantially larger than that of the present study (204 SCZ patients and 212 normal controls), it is possible our failure to reject the null hypothesis for CX3CR1 is related to low statistical power, although this seems unlikely. We did not quantify levels of ADAM17 or cathepsin S, additional fractalkine-modulators, in the present study. However, a previous study found unchanged ADAM17 mRNA levels in postmortem brain tissue in SCZ and BD[142], suggesting its expression is unaltered in either disorder.

In sum, our findings provide evidence of disrupted fractalkine signaling in SCZ, lending further support for an immune role in the pathophysiology of this disorder.

4.1.2 Association Between Fractalkine Signaling and Microglial Parameters is Altered in SCZ

Past research suggests that secretion of fractalkine represses activation of microglia[85,88–91]. As such, deficits in fractalkine signaling may be associated with altered microglial morphology and activation. To this end, we examined potential correlations between levels of fractalkine pathway members and densities of microglia with ramified (‘resting’), non-ramified (‘activated’), or perivascular morphology, quantified in the same subjects as part of a previous study.

We observed positive correlations between CX3CR1 protein and mRNA levels and total microglial density, consistent with reported localization of this protein to microglia. In addition, we found a significant positive association between fractalkine protein levels and total microglial density, as well as density of microglia with a primed/reactive morphology. This was somewhat unexpected, as constitutive expression of fractalkine is believed to repress microglial activation, though this has been demonstrated primarily in neurodegenerative and neuroinflammatory conditions[85]. Nonetheless, there did not appear to be a strong relationship between fractalkine signaling and altered microglial activation status in SCZ.

Rather than relating to microglial activation status, it is possible that impaired fractalkine signaling in SCZ contributes to changes in other microglial parameters. Indeed, fractalkine protein levels negatively correlated with microglial clustering, which we previously found to be increased in SCZ compared to non-psychiatric controls (unpublished data). Hence, under specific circumstances, disruptions in this signal pathway may contribute to changes in spatial distribution of microglia throughout the brain, rather than homeostatic inhibition of microglial activation.

4.1.3 Association Between Fractalkine Signaling and Synaptic Density is Altered in SCZ

Finally, fractalkine signaling has been implicated in mediation of synaptic connectivity, at least in the developing brain[18,132]. As such, we investigated whether fractalkine signaling is associated with synaptic density in SCZ, BD, and MDD. In the control group, protein levels of the fractalkine receptor CX3CR1 were highly correlated with various pre-synaptic proteins,

including SNAP-25, syntaxin, synaptobrevin, Septin 5, complexin I, synaptophysin, synaptotagmin, and complexin II, even after controlling for MBP levels. However, the strength of these correlations was reduced in SCZ. Comparison of the correlation coefficients revealed a statistically significant decrease in the strength of the correlations between CX3CR1 and all pre-synaptic proteins except complexin II in SCZ, relative to the control group. Unexpectedly, the inverse effect was observed for fractalkine mRNA, with fractalkine transcript levels correlated with syntaxin and synaptotagmin protein levels in the SCZ group, but not the control group. So, while expression levels of CX3CR1 protein and fractalkine mRNA did not differ across diagnostic groups, the apparent relation between these measures and pre-synaptic protein levels did.

It is challenging to know how to interpret this observation. Given that we were unable to detect CX3CR1 protein in white matter homogenate, inadvertent inclusion of small amounts of white matter in our samples may contribute to the strong positive correlation with pre-synaptic proteins. However, partial correlation analyses of CX3CR1 and various synaptic proteins, controlling for MBP levels, indicates that the associations are still highly robust in the control group and considerably weaker in the SCZ group. Why expression levels of CX3CR1 and pre-synaptic proteins would be so highly coordinated in normal brain is intriguing. While the present study does not answer this question, it is feasible that CX3CR1 may play a role in microglial maintenance of synapses, with disruptions in this process a feature of SCZ. While microglia undoubtedly carry out numerous functions in the brain, it is possible that fractalkine pathway perturbations contribute to altered microglial distribution throughout the SCZ brain, thereby stifling microglial maintenance of synaptic organization and function.

4.2 Limitations

4.2.1 Potential Confounding Variables Associated with Postmortem Tissue

Obtaining uniform findings in human postmortem studies is extremely challenging due to the range of external variables that may be present in the human lifetime. Factors such as age, sex, PMI, BMI, and brain pH cannot easily be controlled for experimentally, so must be accounted for during statistical analysis. Measures of alcohol and drug use, smoking status, and prescribed medications were available for many subjects in the present study, but not for all individuals. For example, examining the effects of smoking status could not be done in the present study without substantially reducing our sample size. Because individuals with BD and SCZ were more likely to smoke, use alcohol and be prescribed psychotropic medications, these factors could not adequately be controlled for in an ANCOVA model. However, we examined the influence of these factors separately in psychiatric patients, finding effects of antipsychotic drugs on fractalkine levels. As such, the influence of these medications should be considered when interpreting the data. While we did not have data on smoking status for all subjects in the present study, a previous investigation found an effect of smoking on peripheral fractalkine expression; however, smoking was associated with upregulation of fractalkine in the arterial endothelium in this context[143], which is not necessarily reflective of fractalkine levels in brain. We found no evidence of a significant relationship between lifetime alcohol use and mRNA or protein levels of fractalkine or CX3CR1 in the brain in the present study. However, others have found evidence of reduced plasma fractalkine levels in individuals with alcohol use disorders[144]. Finally, we examined the potential link between brain levels of fractalkine pathway members and serum CRP, a marker of peripheral inflammation. Despite increased serum CRP in the SCZ group, we

found no relationship between peripheral inflammation and dysregulation of fractalkine signaling in the brain.

4.2.2 Methodological Limitations

Though widely used in the scientific community, immunoblotting is an imperfect method of measuring relative protein levels. Normalization procedures, in particular, can introduce unintended bias into the results. Our lab has previously observed significant differences in levels of typical reference proteins in BD and SCZ; thus, we opted to normalize instead to total protein detected through the use of Memcode reversible stain. All samples in the present study were loaded in a random order, as determined by the brain bank. The choice of primary antibody may also have considerable influence. For example, while the antibody used for fractalkine detection in the present study has over 30 citations, it is possible that this antibody's binding affinity differs significantly from that of other fractalkine antibodies. This may explain some of the differences reported in the literature with regard to fractalkine's regional distribution and cellular localization.

While ddPCR has several benefits, such as yielding absolute measures for transcript levels at reaction end-point, is nevertheless subject to many of the same confounding variables as conventional qPCR, including sample quality, efficiency of reverse transcription, pipetting errors, primer efficiency, and uniformity of thermal cycler heating. Sample quality may have influenced the ddPCR results in the Array Series, as the average CX3CR1 copy number trended towards the lower limits of detection and was substantially lower than that observed in the Depression Series. This may have contributed to our failure to detect a difference in CX3CR1

mRNA expression, contradicting findings from a prior investigation of CX3CR1 mRNA expression in SCZ[108].

4.3 Future Directions

Several questions remain unanswered by the present study. Establishing the regional distribution and cellular localization of fractalkine and CX3CR1 in the brain in psychiatric disorders is a necessity. Further, additional studies are needed to identify alternative fractalkine cleavage sites and corresponding proteases, as well as the conditions under which they are active. The fractalkine pathway appears to be a highly dynamic mode of neuron-microglia cross-talk that is able to rapidly adjust to circumstances. Characterization of the conditions in which ligand and receptor are upregulated and downregulated is critical. Fractalkine knock-out animals may be useful in deciphering the effects of fractalkine-CX3CR1 signaling on microglial function across various conditions. While the capacity of the fractalkine-CX3CR1 axis to regulate synaptic connections has been explored in developing mice, an analogous function is not yet elucidated in the adult uninjured brain. It is also unclear whether fractalkine signaling is responsible for recruiting microglia to synaptic sites, or merely promotes microglial proliferation throughout the brain parenchyma. Finally, elucidation of the effects of antipsychotic medications on fractalkine protein levels in SCZ will be important for further understanding the chemokine's significance in the disorder. Our lab has tissue from rats administered antipsychotics, or saline control, and comparison of fractalkine levels in these animals would be a worthwhile future direction.

While the findings of the present study add to evidence of a fractalkine-CX3CR1 role in SCZ, there is much to be established before the influence of fractalkine signaling in this disorder is fully understood.

References

1. Häfner, H. *et al.* The Epidemiology of Early Schizophrenia: Influence of Age and Gender on Onset and Early Course. *Br. J. Psychiatry* **164**, 29–38 (1994).
2. Moreno-Küstner, B., Martín, C. & Pastor, L. Prevalence of psychotic disorders and its association with methodological issues. A systematic review and meta-analyses. *PLoS ONE* **13**, (2018).
3. GBD 2016 Disease and Injury Incidence and Prevalence Collaborators. Global, regional, and national incidence, prevalence, and years lived with disability for 328 diseases and injuries for 195 countries, 1990–2016: a systematic analysis for the Global Burden of Disease Study 2016. *Lancet Lond. Engl.* **390**, 1211–1259 (2017).
4. American Psychiatric Association. *Diagnostic and Statistical Manual of Mental Disorders*. (American Psychiatric Association, 2013). doi:10.1176/appi.books.9780890425596
5. Schaffer, A., Cairney, J., Cheung, A., Veldhuizen, S. & Levitt, A. Community Survey of Bipolar Disorder in Canada: Lifetime Prevalence and Illness Characteristics. *Can. J. Psychiatry* **51**, 9–16 (2006).
6. Vieta, E. *et al.* Bipolar disorders. *Nat. Rev. Dis. Primer* **4**, 18008 (2018).
7. Dagani, J. *et al.* Meta-analysis of the Interval between the Onset and Management of Bipolar Disorder. *Can. J. Psychiatry Rev. Can. Psychiatr.* **62**, 247–258 (2017).
8. Otte, C. *et al.* Major depressive disorder. *Nat. Rev. Dis. Primer* **2**, 16065 (2016).
9. *Depression and Other Common Mental Disorders: Global Health Estimates*. (World Health Organization, 2017).
10. Chaplin, D. D. Overview of the Immune Response. *J. Allergy Clin. Immunol.* **125**, S3-23 (2010).

11. Neher, J. J. & Cunningham, C. Priming Microglia for Innate Immune Memory in the Brain. *Trends Immunol.* **40**, 358–374 (2019).
12. Taylor, S. E., Morganti-Kossmann, C., Lifshitz, J. & Ziebell, J. M. Rod Microglia: A Morphological Definition. *PLOS ONE* **9**, e97096 (2014).
13. Streit, W. J., Sammons, N. W., Kuhns, A. J. & Sparks, D. L. Dystrophic microglia in the aging human brain. *Glia* **45**, 208–212 (2004).
14. Faraco, G., Park, L., Anrather, J. & Iadecola, C. Brain perivascular macrophages: characterization and functional roles in health and disease. *J. Mol. Med. Berl. Ger.* **95**, 1143–1152 (2017).
15. Engelhardt, B., Vajkoczy, P. & Weller, R. O. The movers and shapers in immune privilege of the CNS. *Nat. Immunol.* **18**, 123–131 (2017).
16. Medawar, P. B. Immunity to Homologous Grafted Skin. III. The Fate of Skin Homographs Transplanted to the Brain, to Subcutaneous Tissue, and to the Anterior Chamber of the Eye. *Br. J. Exp. Pathol.* **29**, 58–69 (1948).
17. Lynall, M.-E. *et al.* Functional Connectivity and Brain Networks in Schizophrenia. *J. Neurosci.* **30**, 9477–9487 (2010).
18. Paolicelli, R. C. *et al.* Synaptic Pruning by Microglia Is Necessary for Normal Brain Development. *Science* **333**, 1456–1458 (2011).
19. Zhan, Y. *et al.* Deficient neuron-microglia signaling results in impaired functional brain connectivity and social behavior. *Nat. Neurosci.* **17**, 400–406 (2014).
20. Gunner, G. *et al.* Sensory lesioning induces microglial synapse elimination via ADAM10 and fractalkine signaling. *Nat. Neurosci.* **22**, 1075–1088 (2019).

21. Ragozzino, D. *et al.* Chemokine Fractalkine/CX3CL1 Negatively Modulates Active Glutamatergic Synapses in Rat Hippocampal Neurons. *J. Neurosci.* **26**, 10488–10498 (2006).
22. Bertollini, C., Ragozzino, D., Gross, C., Limatola, C. & Eusebi, F. Fractalkine/CX3CL1 depresses central synaptic transmission in mouse hippocampal slices. *Neuropharmacology* **51**, 816–821 (2006).
23. Rogers, J. T. *et al.* CX3CR1 Deficiency Leads to Impairment of Hippocampal Cognitive Function and Synaptic Plasticity. *J. Neurosci.* **31**, 16241–16250 (2011).
24. Heinisch, S. & Kirby, L. G. Fractalkine/CX3CL1 enhances GABA synaptic activity at serotonin neurons in the rat dorsal raphe nucleus. *Neuroscience* **164**, 1210–1223 (2009).
25. Monji, A., Kato, T. & Kanba, S. Cytokines and schizophrenia: Microglia hypothesis of schizophrenia. *Psychiatry Clin. Neurosci.* **63**, 257–265 (2009).
26. Radewicz, K., Garey, L. J., Gentleman, S. M. & Reynolds, R. Increase in HLA-DR Immunoreactive Microglia in Frontal and Temporal Cortex of Chronic Schizophrenics. *J. Neuropathol. Exp. Neurol.* **59**, 137–150 (2000).
27. Steiner, J. *et al.* Distribution of HLA-DR-positive microglia in schizophrenia reflects impaired cerebral lateralization. *Acta Neuropathol. (Berl.)* **112**, 305–316 (2006).
28. Brisch, R. *et al.* Microglia in the dorsal raphe nucleus plays a potential role in both suicide facilitation and prevention in affective disorders. *Eur. Arch. Psychiatry Clin. Neurosci.* **267**, 403–415 (2017).
29. Hercher, C., Chopra, V. & Beasley, C. L. Evidence for morphological alterations in prefrontal white matter glia in schizophrenia and bipolar disorder. *J. Psychiatry Neurosci. JPN* **39**, 376–385 (2014).

30. Kreisl, W. C. *et al.* A genetic polymorphism for translocator protein 18 kDa affects both in vitro and in vivo radioligand binding in human brain to this putative biomarker of neuroinflammation. *J. Cereb. Blood Flow Metab. Off. J. Int. Soc. Cereb. Blood Flow Metab.* **33**, 53–58 (2013).
31. Berckel, B. N. van *et al.* Microglia Activation in Recent-Onset Schizophrenia: A Quantitative (R)-[11C]PK11195 Positron Emission Tomography Study. *Biol. Psychiatry* **64**, 820–822 (2008).
32. Collste, K. *et al.* Lower levels of the glial cell marker TSPO in drug-naive first-episode psychosis patients as measured using PET and [11 C]PBR28. *Mol. Psychiatry* **22**, 850–856 (2017).
33. Notter, T. *et al.* Translational evaluation of translocator protein as a marker of neuroinflammation in schizophrenia. *Mol. Psychiatry* **23**, 323–334 (2018).
34. Hafizi, S. *et al.* Imaging Microglial Activation in Untreated First-Episode Psychosis: A PET Study With [18F]FEPPA. *Am. J. Psychiatry* **174**, 118–124 (2017).
35. Holmes, S. E. *et al. In vivo* imaging of brain microglial activity in antipsychotic-free and medicated schizophrenia: a [^{11}C]*(R)*-PK11195 positron emission tomography study. *Mol. Psychiatry* **21**, 1672–1679 (2016).
36. Lavisse, S. *et al.* Reactive astrocytes overexpress TSPO and are detected by TSPO positron emission tomography imaging. *J. Neurosci. Off. J. Soc. Neurosci.* **32**, 10809–10818 (2012).
37. Pandey, G. N., Rizavi, H. S., Zhang, H. & Ren, X. Abnormal gene and protein expression of inflammatory cytokines in the postmortem brain of schizophrenia patients. *Schizophr. Res.* **192**, 247–254 (2018).

38. Fillman, S. G. *et al.* Increased inflammatory markers identified in the dorsolateral prefrontal cortex of individuals with schizophrenia. *Mol. Psychiatry* **18**, 206–214 (2013).
39. Fillman, S. G., Sinclair, D., Fung, S. J., Webster, M. J. & Shannon Weickert, C. Markers of inflammation and stress distinguish subsets of individuals with schizophrenia and bipolar disorder. *Transl. Psychiatry* **4**, e365 (2014).
40. Volk, D. W. *et al.* Molecular Mechanisms and Timing of Cortical Immune Activation in Schizophrenia. *Am. J. Psychiatry* **172**, 1112–1121 (2015).
41. Harris, L. W. *et al.* Comparison of Peripheral and Central Schizophrenia Biomarker Profiles. *PLOS ONE* **7**, e46368 (2012).
42. Toyooka, K. *et al.* A decrease in interleukin-1 receptor antagonist expression in the prefrontal cortex of schizophrenic patients. *Neurosci. Res.* **46**, 299–307 (2003).
43. García-Bueno, B. *et al.* Evidence of activation of the Toll-like receptor-4 proinflammatory pathway in patients with schizophrenia. *J. Psychiatry Neurosci. JPN* **41**, E46–E55 (2016).
44. Seredenina, T. *et al.* Decreased NOX2 expression in the brain of patients with bipolar disorder: association with valproic acid prescription and substance abuse. *Transl. Psychiatry* **7**, e1206 (2017).
45. Rao, J. S., Harry, G. J., Rapoport, S. I. & Kim, H. W. Increased excitotoxicity and neuroinflammatory markers in postmortem frontal cortex from bipolar disorder patients. *Mol. Psychiatry* **15**, 384–392 (2010).
46. Sneeboer, M. A. M. *et al.* Microglia in post-mortem brain tissue of patients with bipolar disorder are not immune activated. *Transl. Psychiatry* **9**, 1–10 (2019).

47. Nakatani, N. *et al.* Genome-wide expression analysis detects eight genes with robust alterations specific to bipolar I disorder: relevance to neuronal network perturbation. *Hum. Mol. Genet.* **15**, 1949–1962 (2006).

48. Kim, Y.-K., Jung, H.-G., Myint, A.-M., Kim, H. & Park, S.-H. Imbalance between pro-inflammatory and anti-inflammatory cytokines in bipolar disorder. *J. Affect. Disord.* **104**, 91–95 (2007).

49. Ortiz-Domínguez, A. *et al.* Immune variations in bipolar disorder: phasic differences. *Bipolar Disord.* **9**, 596–602 (2007).

50. Knijff, E. M. *et al.* An imbalance in the production of IL-1β and IL-6 by monocytes of bipolar patients: restoration by lithium treatment. *Bipolar Disord.* **9**, 743–753 (2007).

51. Kim, H. K., Andreazza, A. C., Elmi, N., Chen, W. & Young, L. T. Nod-like receptor pyrin containing 3 (NLRP3) in the post-mortem frontal cortex from patients with bipolar disorder: A potential mediator between mitochondria and immune-activation. *J. Psychiatr. Res.* **72**, 43–50 (2016).

52. Dean, B. *et al.* Different changes in cortical tumor necrosis factor-α-related pathways in schizophrenia and mood disorders. *Mol. Psychiatry* **18**, 767–773 (2013).

53. Steiner, J. *et al.* Immunological aspects in the neurobiology of suicide: elevated microglial density in schizophrenia and depression is associated with suicide. *J. Psychiatr. Res.* **42**, 151–157 (2008).

54. Steiner, J. *et al.* Severe depression is associated with increased microglial quinolinic acid in subregions of the anterior cingulate gyrus: evidence for an immune-modulated glutamatergic neurotransmission? *J. Neuroinflammation* **8**, 94 (2011).

55. Torres-Platas, S. G., Cruceanu, C., Chen, G. G., Turecki, G. & Mechawar, N. Evidence for increased microglial priming and macrophage recruitment in the dorsal anterior cingulate white matter of depressed suicides. *Brain. Behav. Immun.* **42**, 50–59 (2014).

56. Holmes, S. E. *et al.* Elevated Translocator Protein in Anterior Cingulate in Major Depression and a Role for Inflammation in Suicidal Thinking: A Positron Emission Tomography Study. *Biol. Psychiatry* **83**, 61–69 (2018).

57. Li, H., Sagar, A. P. & Kéri, S. Microglial markers in the frontal cortex are related to cognitive dysfunctions in major depressive disorder. *J. Affect. Disord.* **241**, 305–310 (2018).

58. Setiawan, E. *et al.* Role of Translocator Protein Density, a Marker of Neuroinflammation, in the Brain During Major Depressive Episodes. *JAMA Psychiatry* **72**, 268–275 (2015).

59. Hannestad, J. *et al.* The neuroinflammation marker translocator protein is not elevated in individuals with mild-to-moderate depression: A [11C]PBR28 PET study. *Brain. Behav. Immun.* **33**, 131–138 (2013).

60. Najjar, S., Pearlman, D. M., Alper, K., Najjar, A. & Devinsky, O. Neuroinflammation and psychiatric illness. *J. Neuroinflammation* **10**, 43 (2013).

61. Yirmiya, R., Rimmerman, N. & Reshef, R. Depression as a Microglial Disease. *Trends Neurosci.* **38**, 637–658 (2015).

62. Biber, K., Neumann, H., Inoue, K. & Boddeke, H. W. G. M. Neuronal 'On' and 'Off' signals control microglia. *Trends Neurosci.* **30**, 596–602 (2007).

63. Uhlén, M. *et al.* Tissue-based map of the human proteome. *Science* **347**, 1260419 (2015).

64. Bazan, J. F. *et al.* A new class of membrane-bound chemokine with a CX3C motif. *Nature* **385**, 640–644 (1997).

65. Hundhausen, C. *et al.* The disintegrin-like metalloproteinase ADAM10 is involved in constitutive cleavage of CX3CL1 (fractalkine) and regulates CX3CL1-mediated cell-cell adhesion. *Blood* **102**, 1186–1195 (2003).

66. Garton, K. J. *et al.* TACE (ADAM17) Mediates the Cleavage and Shedding of Fractalkine (CX3CL1). *J. Biol. Chem.* **276**, (2001).

67. Tsou, C.-L., Haskell, C. A. & Charo, I. F. Tumor Necrosis Factor-α-converting Enzyme Mediates the Inducible Cleavage of Fractalkine. *J. Biol. Chem.* **276**, 44622–44626 (2001).

68. Clark, A. K. *et al.* Inhibition of spinal microglial cathepsin S for the reversal of neuropathic pain. *Proc. Natl. Acad. Sci. U. S. A.* **104**, 10655–10660 (2007).

69. Fonović, U. P., Jevnikar, Z. & Kos, J. Cathepsin S generates soluble CX3CL1 (fractalkine) in vascular smooth muscle cells. *Biol. Chem.* **394**, 1349–1352 (2013).

70. Jones, B. A., Beamer, M. & Ahmed, S. Fractalkine/CX3CL1: A Potential New Target for Inflammatory Diseases. *Mol. Interv.* **10**, 263–270 (2010).

71. Harrison, J. K. *et al.* Role for neuronally derived fractalkine in mediating interactions between neurons and CX3CR1-expressing microglia. *Proc. Natl. Acad. Sci. U. S. A.* **95**, 10896–10901 (1998).

72. Nishiyori, A. *et al.* Localization of fractalkine and CX3CR1 mRNAs in rat brain: does fractalkine play a role in signaling from neuron to microglia? *FEBS Lett.* **429**, 167–172 (1998).

73. Xu, Y. *et al.* Altered Expression of CX3CL1 in Patients with Epilepsy and in a Rat Model. *Am. J. Pathol.* **180**, 1950–1962 (2012).

74. Pan, Y. *et al.* Neurotactin, a membrane-anchored chemokine upregulated in brain inflammation. *Nature* **387**, 611 (1997).

75. Hulshof, S. *et al.* CX3CL1 and CX3CR1 Expression in Human Brain Tissue: Noninflammatory Control versus Multiple Sclerosis. *J. Neuropathol. Exp. Neurol.* **62**, 899–907 (2003).

76. The UniProt Consortium. CX3CL1 - Fractalkine precursor - Homo sapiens (Human) - CX3CL1 gene & protein. *UniProt Knowledgebase* (1999). Available at: https://www.uniprot.org/uniprot/P78423. (Accessed: 18th July 2019)

77. Hermand, P. *et al.* Functional Adhesiveness of the CX3CL1 Chemokine Requires Its Aggregation. *J. Biol. Chem.* **283**, 30225–30234 (2008).

78. Morganti, J. M. *et al.* The Soluble Isoform of CX3CL1 Is Necessary for Neuroprotection in a Mouse Model of Parkinson's Disease. *J. Neurosci.* **32**, 14592–14601 (2012).

79. Muehlhoefer, A. *et al.* Fractalkine Is an Epithelial and Endothelial Cell-Derived Chemoattractant for Intraepithelial Lymphocytes in the Small Intestinal Mucosa. *J. Immunol.* **164**, 3368–3376 (2000).

80. Roche, S. L., Wyse-Jackson, A. C., Ruiz-Lopez, A. M., Byrne, A. M. & Cotter, T. G. Fractalkine-CX3CR1 signaling is critical for progesterone-mediated neuroprotection in the retina. *Sci. Rep.* **7**, 43067 (2017).

81. Zieger, M., Ahnelt, P. K. & Uhrin, P. CX3CL1 (Fractalkine) Protein Expression in Normal and Degenerating Mouse Retina: In Vivo Studies. *PLoS ONE* **9**, (2014).

82. Fong, A. M. *et al.* Ultrastructure and Function of the Fractalkine Mucin Domain in CX3C Chemokine Domain Presentation. *J. Biol. Chem.* **275**, 3781–3786 (2000).

83. Hundhausen, C. *et al.* Regulated Shedding of Transmembrane Chemokines by the Disintegrin and Metalloproteinase 10 Facilitates Detachment of Adherent Leukocytes. *J. Immunol.* **178**, 8064–8072 (2007).

84. Jung, S. *et al.* Analysis of Fractalkine Receptor CX3CR1 Function by Targeted Deletion and Green Fluorescent Protein Reporter Gene Insertion. *Mol. Cell. Biol.* **20**, 4106–4114 (2000).

85. Cardona, A. E. *et al.* Control of microglial neurotoxicity by the fractalkine receptor. *Nat. Neurosci.* **9**, 917–924 (2006).

86. Wollberg, A. R. *et al.* Pharmacological inhibition of the chemokine receptor CX3CR1 attenuates disease in a chronic-relapsing rat model for multiple sclerosis. *Proc. Natl. Acad. Sci.* **111**, 5409–5414 (2014).

87. Pont-Lezica, L. *et al.* Microglia shape corpus callosum axon tract fasciculation: functional impact of prenatal inflammation. *Eur. J. Neurosci.* **39**, 1551–1557 (2014).

88. Zujovic, V., Benavides, J., Vigé, X., Carter, C. & Taupin, V. Fractalkine modulates TNF-alpha secretion and neurotoxicity induced by microglial activation. *Glia* **29**, 305–315 (2000).

89. Zujovic, V., Schussler, N., Jourdain, D., Duverger, D. & Taupin, V. In vivo neutralization of endogenous brain fractalkine increases hippocampal TNFα and 8-isoprostane production induced by intracerebroventricular injection of LPS. *J. Neuroimmunol.* **115**, 135–143 (2001).

90. Mizuno, T., Kawanokuchi, J., Numata, K. & Suzumura, A. Production and neuroprotective functions of fractalkine in the central nervous system. *Brain Res.* **979**, 65–70 (2003).

91. Lyons, A. *et al.* Fractalkine-induced activation of the phosphatidylinositol-3 kinase pathway attentuates microglial activation in vivo and in vitro. *J. Neurochem.* **110**, 1547–1556 (2009).

92. Finneran, D. J. & Nash, K. R. Neuroinflammation and fractalkine signaling in Alzheimer's disease. *J. Neuroinflammation* **16**, 30 (2019).

93. Lee, S. *et al.* CX3CR1 Deficiency Alters Microglial Activation and Reduces Beta-Amyloid Deposition in Two Alzheimer's Disease Mouse Models. *Am. J. Pathol.* **177**, 2549–2562 (2010).

94. Fuhrmann, M. *et al.* Microglial Cx3cr1 knockout prevents neuron loss in a mouse model of Alzheimer's disease. *Nat. Neurosci.* **13**, 411–413 (2010).

95. Soriano, S. G. *et al.* Mice deficient in fractalkine are less susceptible to cerebral ischemia-reperfusion injury. *J. Neuroimmunol.* **125**, 59–65 (2002).

96. Dénes, Á., Ferenczi, S., Halász, J., Környei, Z. & Kovács, K. J. Role of CX3CR1 (Fractalkine Receptor) in Brain Damage and Inflammation Induced by Focal Cerebral Ischemia in Mouse. *J. Cereb. Blood Flow Metab.* **28**, 1707–1721 (2008).

97. Bhaskar, K. *et al.* Regulation of Tau Pathology by the Microglial Fractalkine Receptor. *Neuron* **68**, 19–31 (2010).

98. Cho, S.-H. *et al.* CX3CR1 Protein Signaling Modulates Microglial Activation and Protects against Plaque-independent Cognitive Deficits in a Mouse Model of Alzheimer Disease. *J. Biol. Chem.* **286**, 32713–32722 (2011).

99. Clark, A. K. & Malcangio, M. Microglial signalling mechanisms: Cathepsin S and Fractalkine. *Exp. Neurol.* **234**, 283–292 (2012).

100. Febinger, H. Y. *et al.* Time-dependent effects of CX3CR1 in a mouse model of mild traumatic brain injury. *J. Neuroinflammation* **12**, 154 (2015).

101. Boddeke, E. W. G. M. *et al.* Functional expression of the fractalkine (CX3C) receptor and its regulation by lipopolysaccharide in rat microglia. *Eur. J. Pharmacol.* **374**, 309–313 (1999).

102. Meucci, O. *et al.* Chemokines regulate hippocampal neuronal signaling and gp120 neurotoxicity. *Proc. Natl. Acad. Sci.* **95**, 14500–14505 (1998).

103. Limatola, C. *et al.* Chemokine CX3CL1 protects rat hippocampal neurons against glutamate-mediated excitotoxicity. *J. Neuroimmunol.* **166**, 19–28 (2005).

104. Scianni, M. *et al.* Fractalkine (CX3CL1) enhances hippocampal N-methyl-d-aspartate receptor (NMDAR) function via d-serine and adenosine receptor type A2 (A2AR) activity. *J. Neuroinflammation* **10**, 876 (2013).

105. Tarozzo, G. *et al.* Fractalkine protein localization and gene expression in mouse brain. *J. Neurosci. Res.* **73**, 81–88 (2003).

106. Roseti, C. *et al.* Fractalkine/CX3CL1 modulates GABAA currents in human temporal lobe epilepsy. *Epilepsia* **54**, 1834–1844 (2013).

107. Ishizuka, K. *et al.* Rare genetic variants in CX3CR1 and their contribution to the increased risk of schizophrenia and autism spectrum disorders. *Transl. Psychiatry* **7**, e1184 (2017).

108. Bergon, A. *et al.* CX3CR1 is dysregulated in blood and brain from schizophrenia patients. *Schizophr. Res.* **168**, 434–443 (2015).

109. Padmos, R. C. *et al.* A Discriminating Messenger RNA Signature for Bipolar Disorder Formed by an Aberrant Expression of Inflammatory Genes in Monocytes. *Arch. Gen. Psychiatry* **65**, 395–407 (2008).

110. Hellwig, S. *et al.* Altered microglia morphology and higher resilience to stress-induced depression-like behavior in CX3CR1-deficient mice. *Brain. Behav. Immun.* **55**, 126–137 (2016).

111. Torrey, E. F., Webster, M., Knable, M., Johnston, N. & Yolken, R. H. The Stanley Foundation brain collection and Neuropathology Consortium. *Schizophr. Res.* **44**, 151–155 (2000).

112. The Stanley Neuropathology Consortium Integrative Database. Available at: http://sncid.stanleyresearch.org/Default.aspx?ReturnUrl=%2f. (Accessed: 4th July 2019)

113. R Core Team. *R: A Language and Environment for Statistical Computing*. (R Foundation for Statistical Computing, 2019).

114. Diedenhofen, B. & Musch, J. cocor: A Comprehensive Solution for the Statistical Comparison of Correlations. *PLOS ONE* **10**, e0121945 (2015).

115. Kim, S. ppcor: An R Package for a Fast Calculation to Semi-partial Correlation Coefficients. *Commun. Stat. Appl. Methods* **22**, 665–674 (2015).

116. Wei, T. & Simko, V. *R package 'corrplot': Visualization of a Correlation Matrix*. (2017).

117. Jiang, T. *et al.* Physical Exercise Improves Cognitive Function Together with Microglia Phenotype Modulation and Remyelination in Chronic Cerebral Hypoperfusion. *Front. Cell. Neurosci.* **11**, (2017).

118. Lana, D., Ugolini, F., Nosi, D., Wenk, G. L. & Giovannini, M. G. Alterations in the Interplay between Neurons, Astrocytes and Microglia in the Rat Dentate Gyrus in Experimental Models of Neurodegeneration. *Front. Aging Neurosci.* **9**, (2017).

119. Lucas, A. D. *et al.* The Transmembrane Form of the CX3CL1 Chemokine Fractalkine Is Expressed Predominantly by Epithelial Cells in Vivo. *Am. J. Pathol.* **158**, 855–866 (2001).

120. Ruchaya, P. J., Paton, J. F. R., Murphy, D. & Yao, S. T. A cardiovascular role for fractalkine and its cognate receptor, CX3CR1, in the rat nucleus of the solitary tract. *Neuroscience* **209**, 119–127 (2012).

121. Morari, J. *et al.* Fractalkine (CX3CL1) Is Involved in the Early Activation of Hypothalamic Inflammation in Experimental Obesity. *Diabetes* **63**, 3770–3784 (2014).

122. Liu, Z. *et al.* Fractalkine/CX3CR1 Contributes to Endometriosis-Induced Neuropathic Pain and Mechanical Hypersensitivity in Rats. *Front. Cell. Neurosci.* **12**, (2018).

123. Held-Feindt, J. *et al.* CX3CR1 promotes recruitment of human glioma-infiltrating microglia/macrophages (GIMs). *Exp. Cell Res.* **316**, 1553–1566 (2010).

124. Kim, M., Rooper, L., Xie, J., Kajdacsy-Balla, A. A. & Barbolina, M. V. Fractalkine Receptor CX3CR1 Is Expressed in Epithelial Ovarian Carcinoma Cells and Required for Motility and Adhesion to Peritoneal Mesothelial Cells. *Mol. Cancer Res.* **10**, 11–24 (2012).

125. Lucas Andrew D. *et al.* Smooth Muscle Cells in Human Atherosclerotic Plaques Express the Fractalkine Receptor CX3CR1 and Undergo Chemotaxis to the CX3C Chemokine Fractalkine (CX3CL1). *Circulation* **108**, 2498–2504 (2003).

126. Schäfer, A. *et al.* Novel role of the membrane-bound chemokine fractalkine in platelet activation and adhesion. *Blood* **103**, 407–412 (2004).

127. Anders, A., Gilbert, S., Garten, W., Postina, R. & Fahrenholz, F. Regulation of the α-secretase ADAM10 by its prodomain and proprotein convertases. *FASEB J.* **15**, 1837–1839 (2001).

128. Dittmer, A., Hohlfeld, K., Lützkendorf, J., Müller, L. P. & Dittmer, J. Human mesenchymal stem cells induce E-cadherin degradation in breast carcinoma spheroids by activating ADAM10. *Cell. Mol. Life Sci.* **66**, 3053–3065 (2009).

129. Gutwein, P. *et al.* ADAM10-mediated cleavage of L1 adhesion molecule at the cell surface and in released membrane vesicles. *FASEB J.* **17**, 292–294 (2002).

130. Arnoux, I. & Audinat, E. Fractalkine Signaling and Microglia Functions in the Developing Brain. *Neural Plast.* **2015**, (2015).

131. Ransohoff, R. M. & Perry, V. H. Microglial Physiology: Unique Stimuli, Specialized Responses. *Annu. Rev. Immunol.* **27**, 119–145 (2009).

132. Kettenmann, H., Kirchhoff, F. & Verkhratsky, A. Microglia: New Roles for the Synaptic Stripper. *Neuron* **77**, 10–18 (2013).

133. Chen, Y. A. & Scheller, R. H. SNARE-mediated membrane fusion. *Nat. Rev. Mol. Cell Biol.* **2**, 98–106 (2001).

134. Anand, A., Li, Y., Wang, Y., Lowe, M. J. & Dzemidzic, M. Resting state corticolimbic connectivity abnormalities in unmedicated bipolar disorder and unipolar depression. *Psychiatry Res. Neuroimaging* **171**, 189–198 (2009).

135. Honer, W. G. *et al.* Synaptic and plasticity-associated proteins in anterior frontal cortex in severe mental illness. *Neuroscience* **91**, 1247–1255 (1999).

136. NCBI Resource Coordinators. Database resources of the National Center for Biotechnology Information. *Nucleic Acids Res.* **46**, D8–D13 (2018).

137. Hindson, B. J. *et al.* High-Throughput Droplet Digital PCR System for Absolute Quantitation of DNA Copy Number. *Anal. Chem.* **83**, 8604–8610 (2011).

138. Pinheiro, L. B. *et al.* Evaluation of a Droplet Digital Polymerase Chain Reaction Format for DNA Copy Number Quantification. *Anal. Chem.* **84**, 1003–1011 (2012).

139. Taylor, S. C., Laperriere, G. & Germain, H. Droplet Digital PCR versus qPCR for gene expression analysis with low abundant targets: from variable nonsense to publication quality data. *Sci. Rep.* **7**, 1–8 (2017).

140. Vandesompele, J. Digital PCR for copy number analysis. (2015).

141. Huang, Y.-W. *et al.* Constitutive endocytosis of the chemokine CX3CL1 prevents its degradation by cell surface metalloproteases. *J. Biol. Chem.* **284**, 29644–29653 (2009).

142. Hoseth, E. Z. *et al.* A Study of TNF Pathway Activation in Schizophrenia and Bipolar Disorder in Plasma and Brain Tissue. *Schizophr. Bull.* **43**, 881–890 (2017).

143. Rius, C. *et al.* Critical role of fractalkine (CX3CL1) in cigarette smoke-induced mononuclear cell adhesion to the arterial endothelium. *Thorax* **68**, 177–186 (2013).

144. García-Marchena, N. *et al.* Plasma Chemokines in Patients with Alcohol Use Disorders: Association of CCL11 (Eotaxin-1) with Psychiatric Comorbidity. *Front. Psychiatry* **7**, (2017).

Appendices

Appendix A ddPCR and Immunoblotting Test Results

A.1 ddPCR Replicate Plots

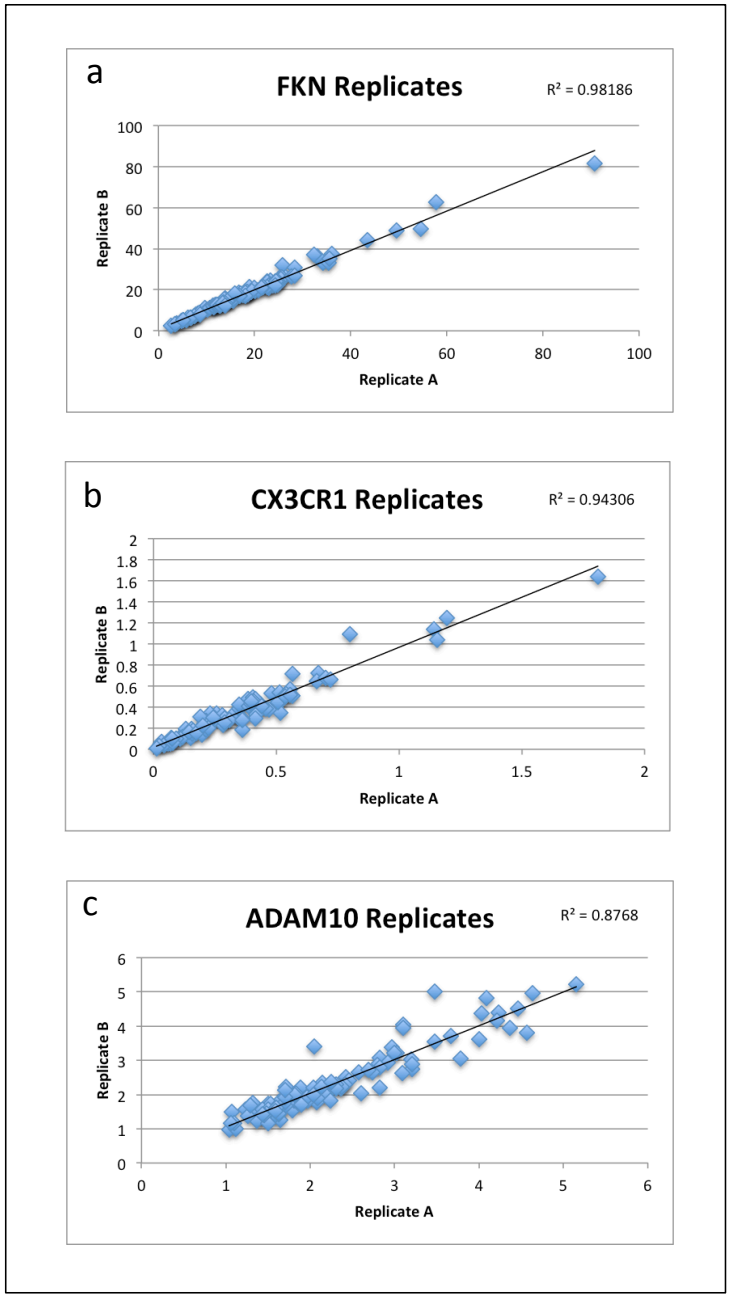

Figure 14: Plots of ddPCR replicate values in the Array Collection.

Relative copy numbers across two replicates for (a) fractalkine (FKN), (b) CX3CR1, and (c) ADAM10.

A.2 Fractalkine Immunoblotting Test Images

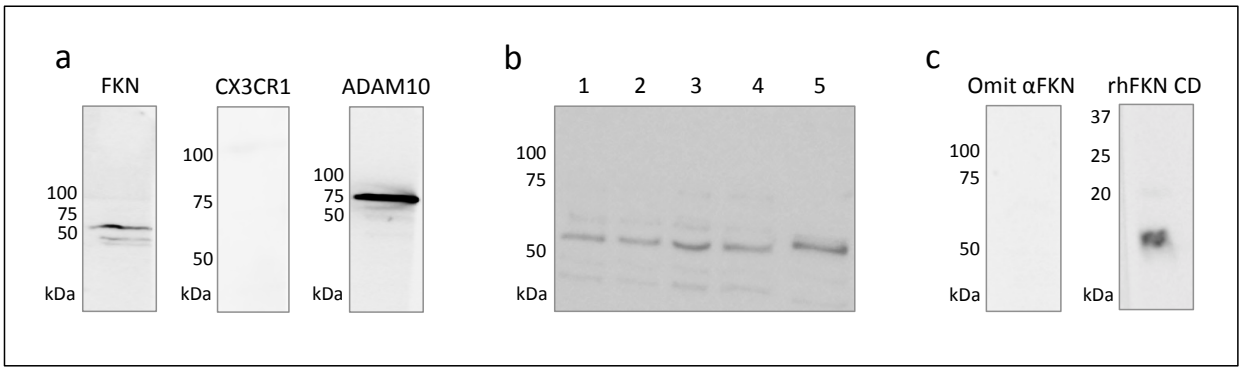

Figure 15: Immunoblotting test images.

(a) White matter homogenates containing pooled test sample from all Array Collection individuals. The fractalkine and ADAM10 white matter lanes were run on a 12% polyacrylamide gel, while the CX3CR1 white matter lane was run on a 10% gel. (b) Results from test of fractalkine degradation product. Immunoblotting for fractalkine was carried out using samples across various conditions: cortical rat tissue left at room temperature for 2 hours following sacrifice of the animal (lane 1); cortical rat tissue left at room temperature for 1 hour following sacrifice (lane 2); cortical rat tissue frozen immediately after sacrifice (lane 3); cortical rat tissue stored at -80°C for several years (lane 5); human DLPFC tissue stored at -80°C for several years (lane 5). All sample conditions yielded a prominent band at ~55Da following immunostaining. (c) Omission of the anti-fractalkine antibody ('Omit αFKN') resulted in no detectable protein bands, while immunoblotting with a recombinant human peptide corresponding to the fractalkine chemokine domain ('rhFKN CD') yielded a prominent band at ~9kDa.

A.3 Example of ddPCR Output

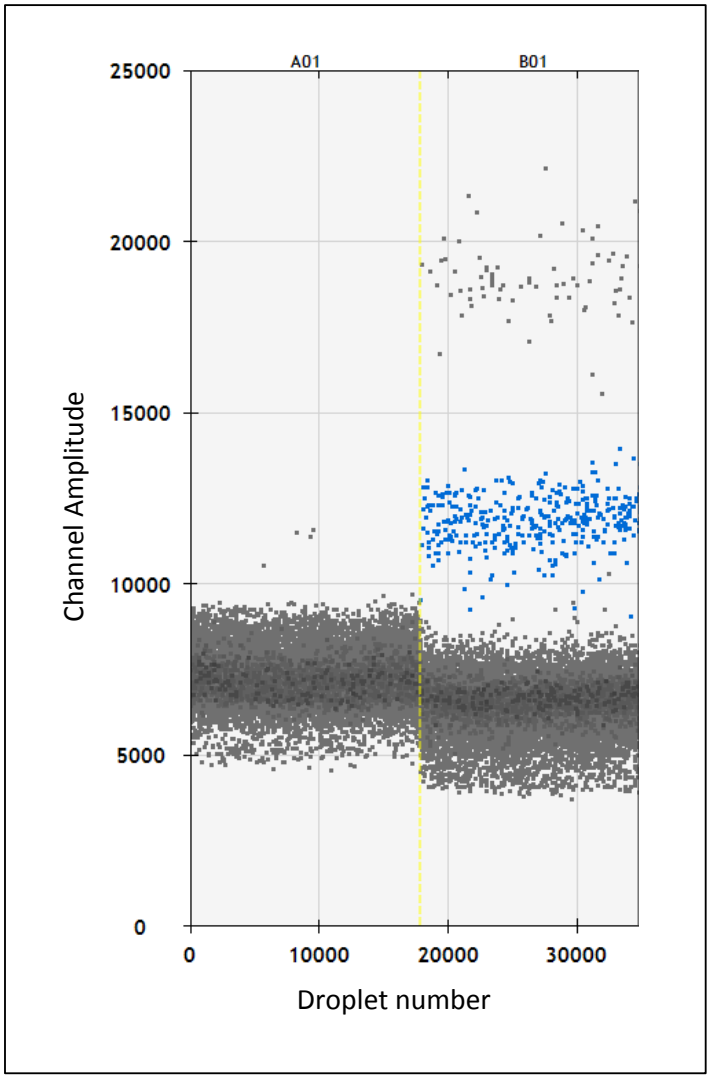

Figure 16: Example of ddPCR droplet clusters in a duplexed assay.

The left column depicts output of a 'no template control', while the right column depicts clusters for ADAM10 (blue cluster) and CX3CR1 (top grey cluster) gene targets.

Appendix B Detailed Statistical Results from Analysis of CX3CR1 and Pre-Synaptic Protein Levels in the Array Collection

B.1 Calculation and Comparison of Spearman Correlations between CX3CR1 and Pre-Synaptic Proteins

	Overall[#]	CON[#]	SCZ[#]	BD[#]	SCZ vs. CON[^]	BD vs. CON[^]
syntaxin (SP6)	**ρ=0.604 p=1.17e-11**	**ρ=0.761 p=1.13e-7**	**ρ=0.381 p=0.024**	**ρ=0.588 p=2.57e-4**	**z=2.39 p=0.0085**	z=1.28 p=0.099
synaptobrevin (SP10)	**ρ=0.434 p=4.23e-06**	**ρ=0.684 p=5.92e-06**	ρ=0.168 p=0.334	**ρ=0.369 p=0.032**	**z=2.67 p=0.004**	**z=1.78 p=0.037**
Septin 5 (SP18)	**ρ=0.497 p=7.93e-08**	**ρ=0.707 p=2.03e-06**	**ρ=0.382 p=0.024**	ρ=0.336 p=0.052	**z=1.92 p=0.027**	**z=2.11 p=0.017**
complexin I (SP33)	**ρ=0.618 p=2.83e-12**	**ρ=0.743 p=3.19e-07**	**ρ=0.503 p=0.002**	**ρ=0.510 p=0.002**	z=1.62 p=0.053	z=1.56 p=0.059
synaptophysin (EP10)	**ρ=0.518 p=1.72e-08**	**ρ=0.721 p=1.02e-06**	ρ=0.258 p=0.135	**ρ=0.495 p=0.003**	**z=2.59 p=0.005**	z=1.46 p=0.073
synaptotagmin (MAb30)	**ρ=0.570 p=2.81e-10**	**ρ=0.749 p=2.27e-07**	**ρ=0.434 p=0.009**	**ρ=0.522 p=0.002**	**z=2.02 p=0.022**	z=1.55 p=0.060
complexin II (LP27)	**ρ=0.525 p=1.06e-08**	**ρ=0.643 p=3.07e-05**	**ρ=0.487 p=0.003**	**ρ=0.454 p=0.007**	z=0.929 p=0.177	z=1.09 p=0.138

Table 4: Correlations between CX3CR1 and pre-synaptic protein levels in the Array Series.

(#) Spearman correlations between protein levels of CX3CR1 and syntaxin (clone SP6), synaptobrevin (clone SP10), Septin 5 (clone SP18), complexin I (clone SP33), synaptophysin (clone EP10), synaptotagmin (clone MAb30), and complexin II (clone LP27) across the entire Array Series ('Overall') or within diagnostic groups.

(^) Test of comparison between Spearman correlation coefficients through Fisher Z-transformation. Findings significant at $p<0.05$ are in bold.

B.2 Spearman Partial Correlations between CX3CR1 and Pre-Synaptic Proteins, Adjusted for MBP

	Overall	CON	SCZ	BD
syntaxin (SP6)	**ρ=0.460 p=1.00e-06**	**ρ=0.667 p=1.63e-05**	ρ=0.240 p=0.172	**ρ=0.373 p=0.033**
synaptobrevin (SP10)	**ρ=0.264 p=0.007**	**ρ=0.518 p=0.002**	ρ=0.059 p=0.739	ρ=0.161 p=0.371
Septin 5 (SP18)	**ρ=0.341 p=4.32e-04**	**ρ=0.570 p=4.32e-04**	ρ=0.295 p=0.091	ρ=0.080 p=0.659
complexin I (SP33)	**ρ=0.430 p=5.74e-06**	**ρ=0.598 p=1.87e-04**	**ρ=0.400 p=0.019**	ρ=0.199 p=0.267
synaptophysin (EP10)	**ρ=0.345 p=3.63e-04**	**ρ=0.598 p=1.86e-04**	ρ=0.081 p=0.649	ρ=0.263 p=0.140
synaptotagmin (MAb30)	**ρ=0.402 p=2.61e-05**	**ρ=0.642 p=4.25e-05**	ρ=0.265 p=0.130	ρ=0.295 p=0.096
complexin II (LP27)	**ρ=0.288 p=0.003**	**ρ=0.437 p=0.010**	ρ=0.306 p=0.078	ρ=0.112 p=0.536

Table 5: Partial correlations between CX3CR1 and pre-synaptic-associated protein levels in the Array Series.

Spearman partial correlations between CX3CR1 and pre-synaptic protein levels, holding levels of MBP constant. Findings significant at $p<0.05$ are in bold.